Methyl side-groups control the $Ia\bar{3}d$ phase in core-non-symmetric aryloyl-hydrazine-based molecules

Sota Takebe,[a] Nachia Isobe,[a] Taro Udagawa,[b] Yasuhisa Yamamura,[c] Kazuya Saito,[d,e] Yohei Miwa,[b] Kei Hashimoto,[b] and Shoichi Kutsumizu[b,*]

[a]*Materials Chemistry Course, Department of Materials Science and Processing, Graduate School of Natural Science and Technology, Gifu University, Yanagido, Gifu 501-1193, Japan.*

[b]*Department of Chemistry and Biomolecular Science, Faculty of Engineering, Gifu University, Yanagido, Gifu 501-1193, Japan.*

[c]*Department of Chemistry, Faculty of Pure and Applied Sciences, University of Tsukuba, Tsukuba, Ibaraki 305-8571, Japan.*

[d]*Center for Computational Sciences, University of Tsukuba, Tsukuba, Ibaraki, 305-8577, Japan.*

[e]*Research Center for Thermal and Entropic Science, Graduate School of Science, Osaka University, Toyonaka, Osaka 560-0043, Japan.*

Contents:

1. **DSC**
2. **POM textures**
3. **XRD**
4. **Molecular structure and electron density map for single molecules based on DFT calculations**
5. **Electron density map based on MEM analyses**
6. **IR**
7. **Interaction energy calculation based on quantum chemical calculations and NCI analysis**
8. **Synthetic details for B-MPB-22, MB-PB-22, and MB-MPB-22**

References for SI

1. DSC

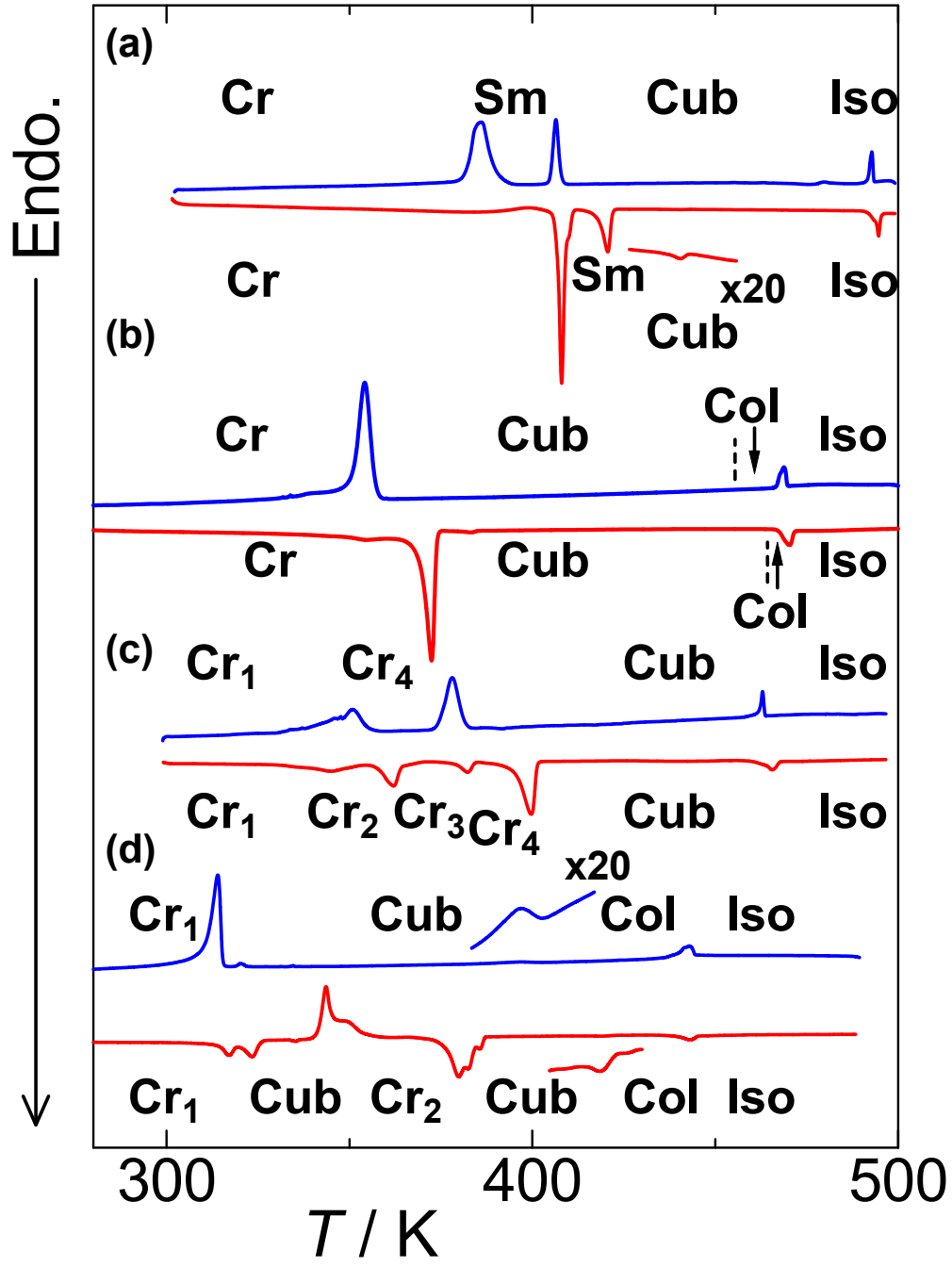

Figure S1. DSC thermograms of (a) B-PB-22,[S1] (b) B-MPB-22, (c) MB-PB-22, and (d) MB-MPB-22 on 1st cooling (——) and 2nd heating (——) at 5 K min^{-1}.

Table S1. Mesophases, transition temperatures (T / K as peak temperatures) and associated enthalpy changes (ΔH / kJ mol^{-1} in brackets) of compounds examined on 1st cooling (1C) and 2nd heating (2H) by DSC (5 K min^{-1}).

Compd.	Phase transitions
B-PB-22[S1]	1C: Cr 386.0 [-103.3] SmF/I 406.6 [-27.2] Cub$^{[*]}$/$I2_13$ [-] Cub/*Ia3d* 492.9 [-6.5] Iso
	2H: Cr 408.1 [76.5] SmF/I 420.7 [24.8] Cub/$I2_13$ 442.1 [0.2] Cub/*Ia3d* 494.7 [7.4] Iso
B-MPB-22	1C: Cr 354.3 [-118.5] Cub/*Ia3d* 455.4[a] [-] Col_h 468.9 [-7.2] Iso
	2H: Cr 372.5 [124.4] Cub/*Ia3d* 464.3[a] [-] Col_h 470.2 [6.8] Iso
MB-PB-22	1C: Cr_1 350.8 [-40.6] Cr_4 378.2 [-36.6] Cub/*Ia3d* 462.9 [-4.8] Iso
	2H: Cr_1 344.9 [11.2] Cr_2 362.0 [16.3] Cr_3 382.3 [5.9] Cr_4 399.8 [36.1] Cub/*Ia3d* 465.5 [7.0] Iso
MB-MPB-22	1C: Cr_1 314.0 [-61.8] Cub/*Ia3d* 393.9 [-1.5] Col_h 443.0 [-18.1] Iso
	2H: Cr_1 317.0 [66.5] Cub/*Ia3d* 343.7 [-106.4] Cr_2 379.9 [107.3] Cub/*Ia3d* 418.7 [0.6] Col_h 443.0 [9.6] Iso

[a] determined by POM observation.

Abbreviation: Cr = crystalline solid; *Ia3d* = cubic (Cub) LC phase with *Ia3d* symmetry; $I2_13$ = chiral cubic (Cub$^{[*]}$) LC phase with a possible symmetry of $I2_13$ symmetry; Col_h = columnar LC phase with a hexagonal lattice; Sm = smectic LC phase; Iso = isotropic liquid; Phase identification was made by DSC, POM, and XRD; for DSCs, see Figure S1, for POM textures, see Figures S2-S8, and for XRD data, see Figures S9-S11 and Tables S2-S5 in this SI.

2. POM textures

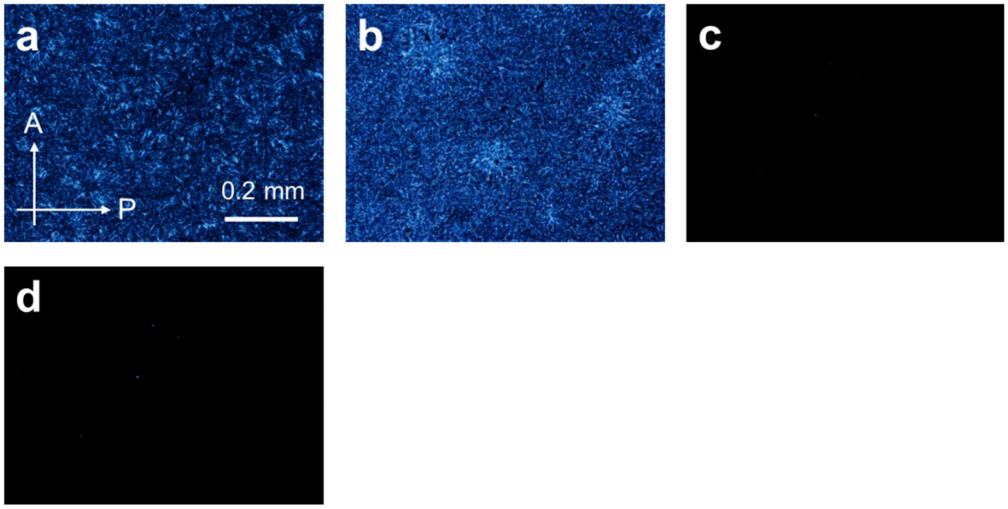

Figure S2. Textures of B-PB-22 at (a) 303.2 K (Cr), (b) 413.2 K (SmF/I) (with poor fluidity), (c) 428.2 K (Cub) and (d) 483.2 K (Cub) on heating (5 K min^{-1}).

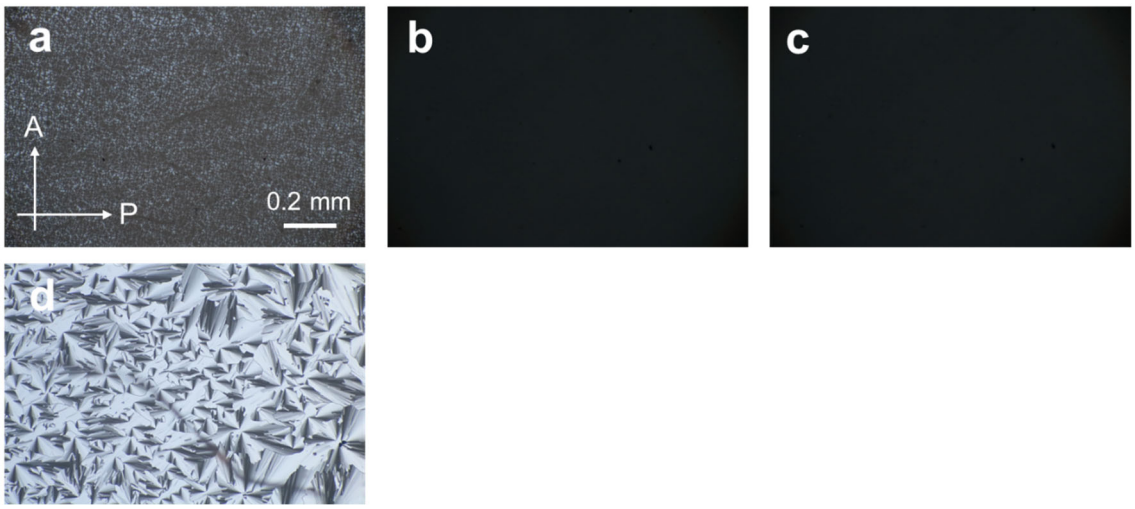

Figure S3. Textures of **B-MPB-22** at (a) 302.2 K (Cr), (b) 380.2 K (Cub), (c) 408.3 K (Cub), and (d) 465.2 K (Col) on heating (5 K min^{-1}).

Figure S4. Textures of B-MPB-22 at (a) 460.1 K (Col), (b) 414.5 K (Cub), and (c) 328.3 K (Cr) on cooling (5 K min^{-1}).

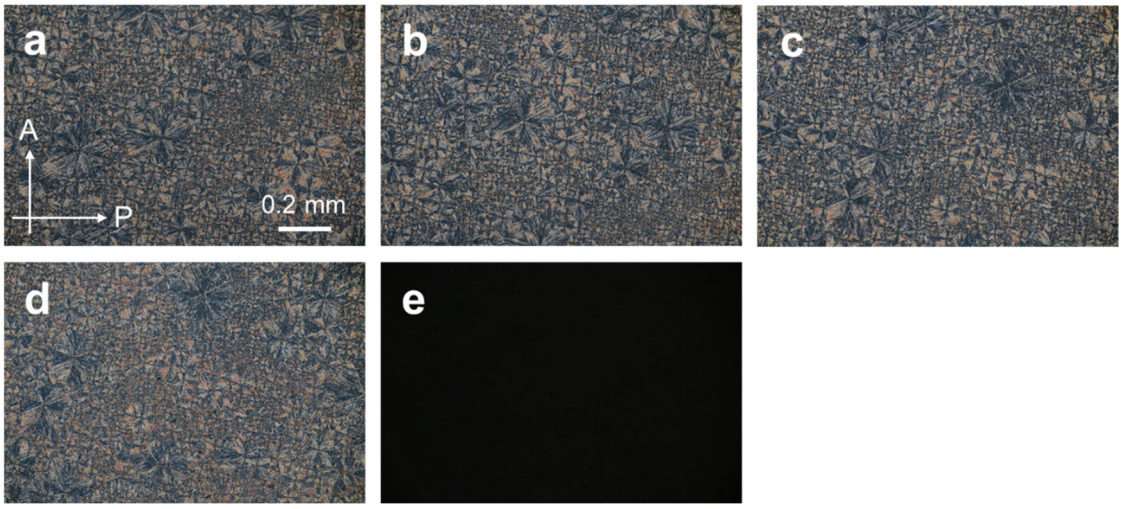

Figure S5. Textures of MB-PB-22 at (a) 303.7 K (Cr_1), (b) 353.1 K (Cr_2), (c) 371.3 K (Cr_3), (d) 390.6 K (Cr_4), and (e) 411.8 K (Cub) on heating (5 K min^{-1}).

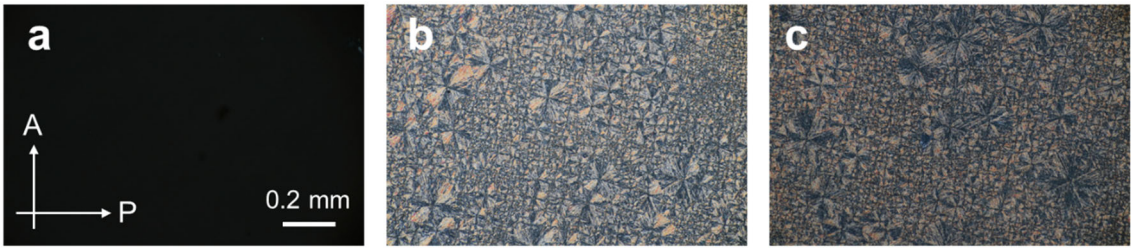

Figure S6. Textures of MB-PB-22 at (a) 432.9 K (Cub), (b) 368.3 K (Cr_4), and (c) 324.3 K (Cr_1) on cooling (5 K min^{-1}).

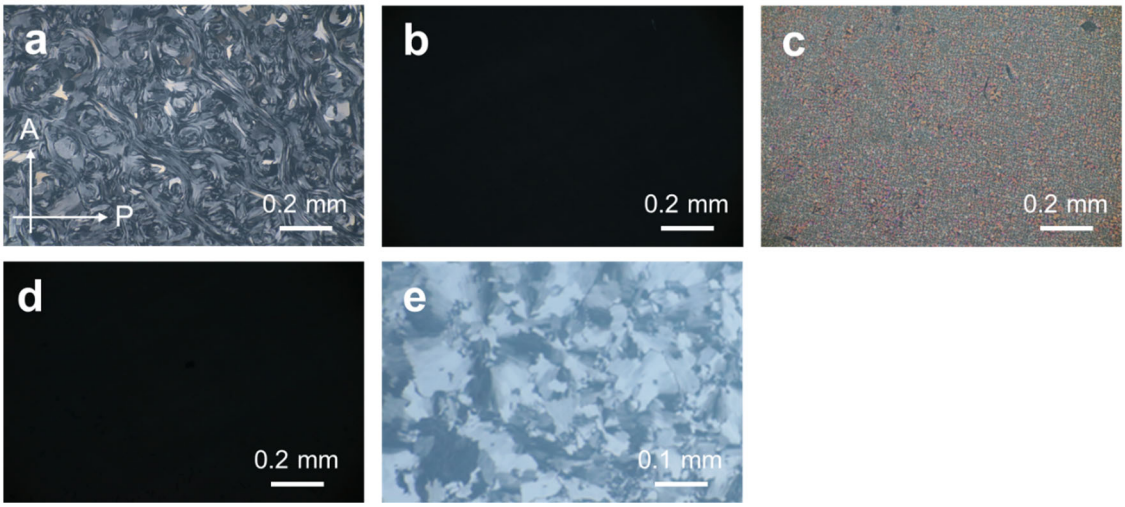

Figure S7. Textures of MB-MPB-22 at (a) 298.1 K (Cr_1), (b) 324.6 K (Cub), (c) 354.1 K (Cr_2), (d) 400.1 K (Cub), and (e) 433.8 K (Col) on heating (5 K min^{-1}).

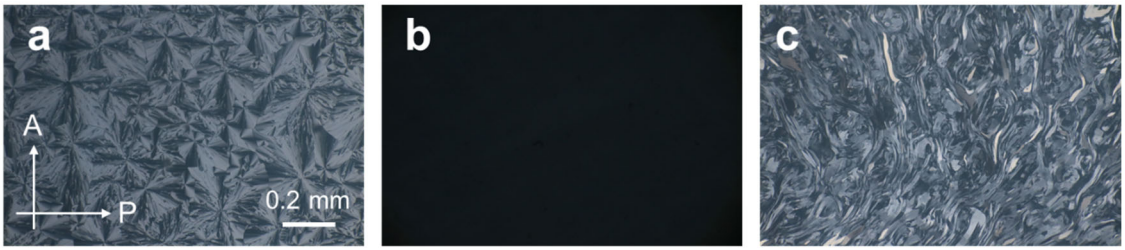

Figure S8. Textures of MB-MPB-22 at (a) 429.7 K (Col), (b) 369.3 K (Cub), and (c) 305.8 K (Cr_1) on cooling (5 K min^{-1}).

3. XRD

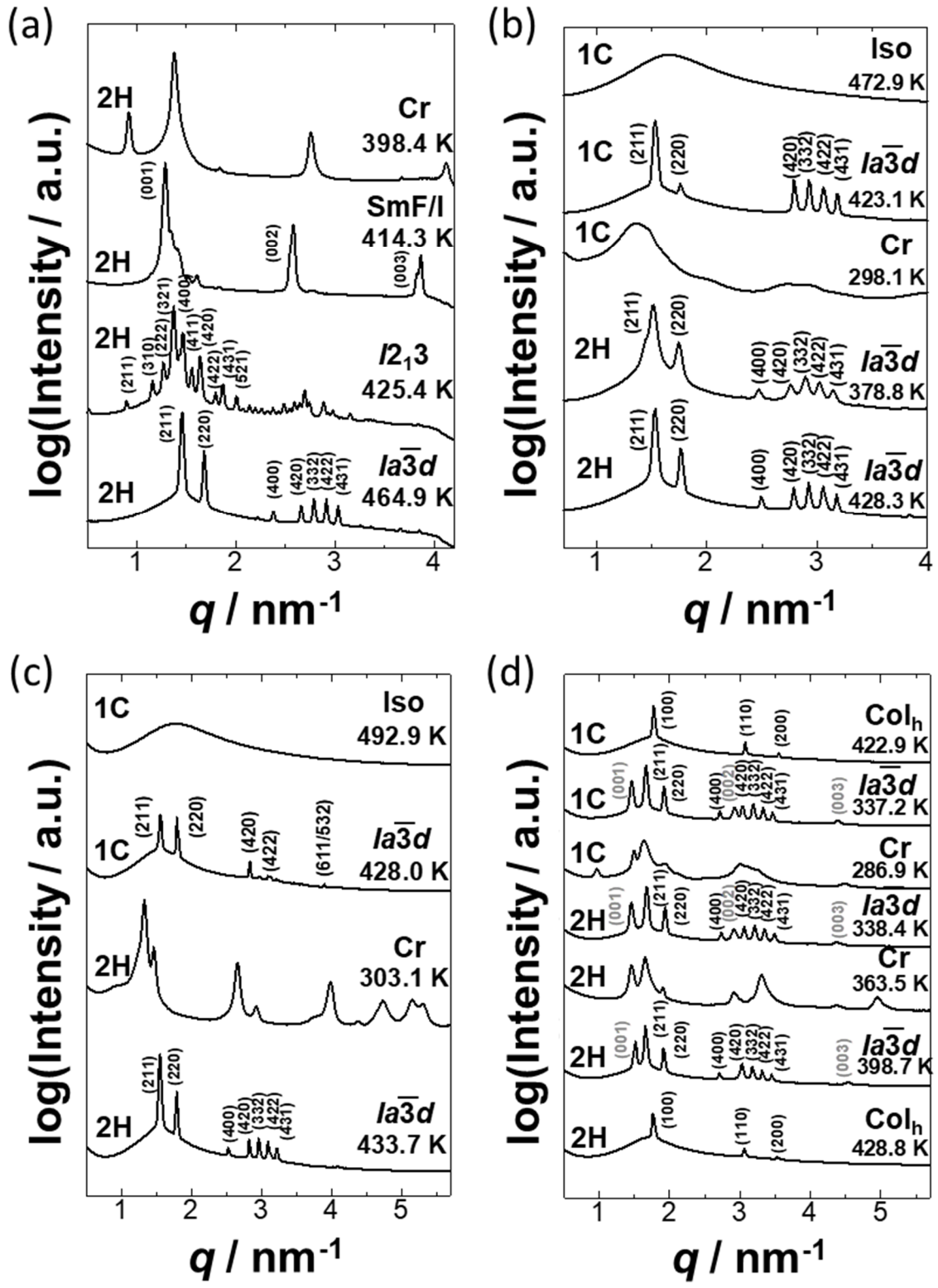

Figure S9. SAXS patterns of (a) B-PB-22, (b) B-MPB-22, (c) MB-PB-22, and (d) MB-MPB-22 on 1st cooling (1C) and 2nd heating (2H) (5 K min^{-1}).

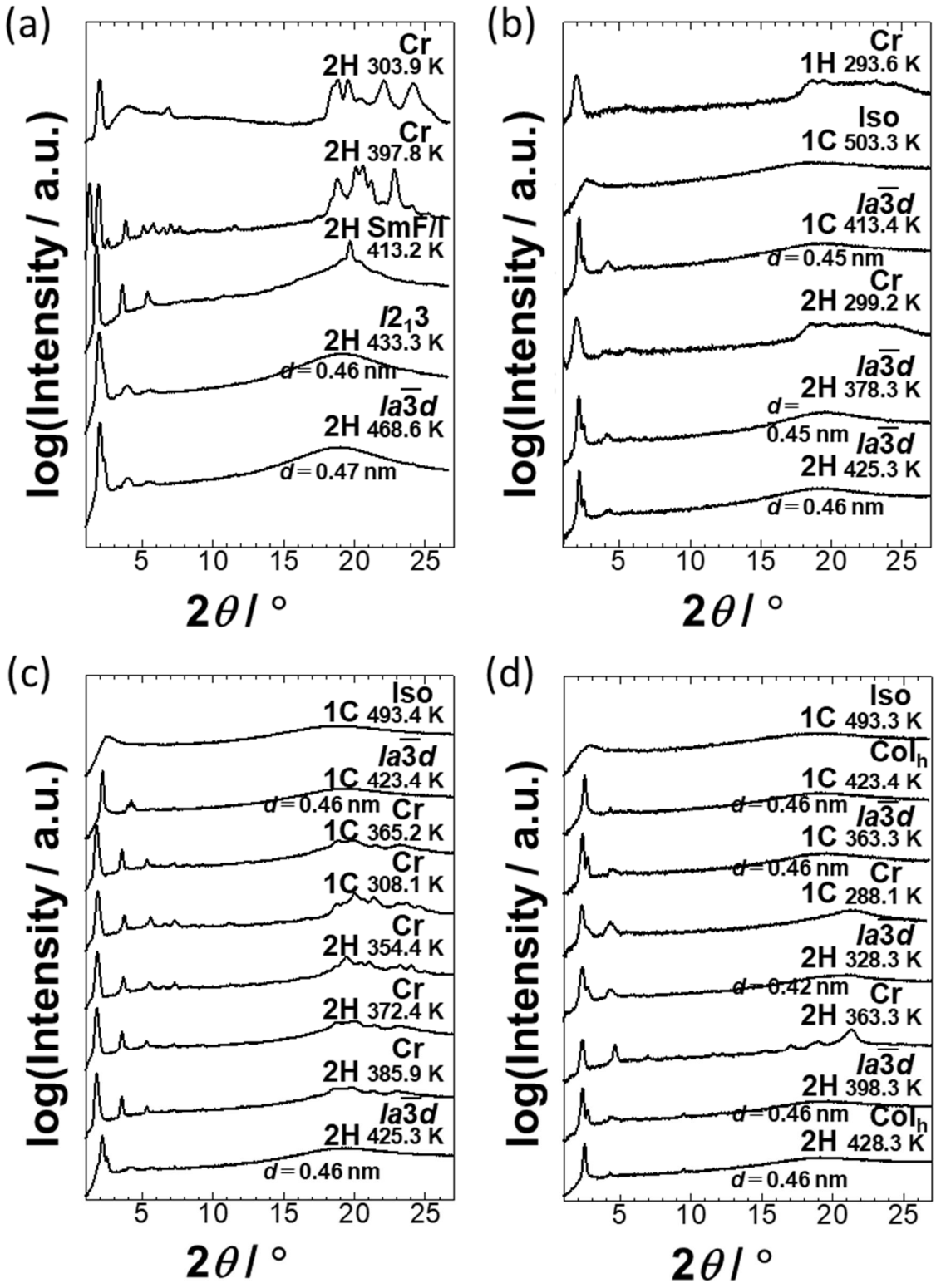

Figure S10. WAXS patterns of (a) B-PB-22, (b) B-MPB-22, (c) MB-PB-22, and (d) MB-MPB-22 on 1st heating (1H), 1st cooling (1C), and 2nd heating (2H).

Table S2. Experimental and calculated 2θ in the WAXS pattern for the SmF/I phase of B-PB-22 at 413.4 K on 1st heating (5 K min^{-1}) given in Figure S10a.

SmF/I with layer spacing L = 4.93±0.02 nm at 413.4 K on heating				
(hkl)	$2\theta_{obs}$ / °	$2\theta_{calc}$ / °	d_{obs} / nm	d_{calc} / nm
(001)	1.781	1.792	4.961	4.930
(002)	3.593	3.584	2.459	2.465
(003)	5.398	5.378	1.637	1.643
(006)	10.816	10.767	0.818	0.822
(100)	19.651		0.452	

The layer spacing L is less than the molecular length, indicating the molecular tilt with respect to the layer normal.

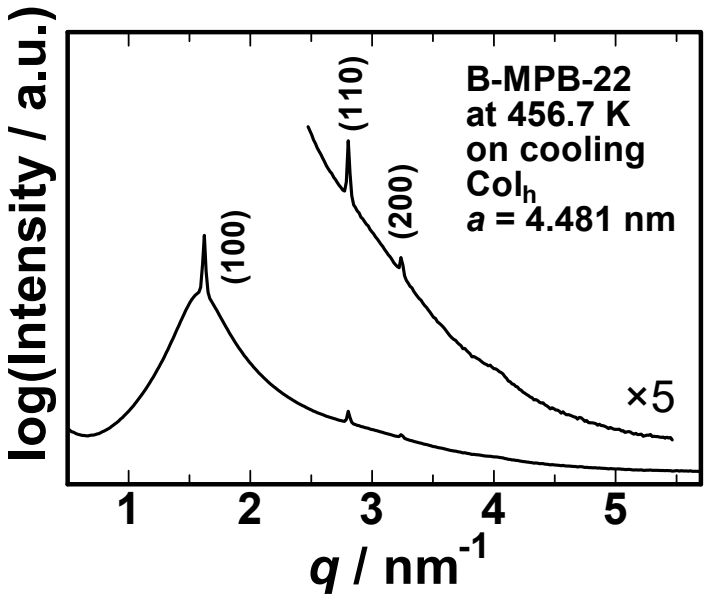

Figure S11. SAXS patterns of B-MPB-22 at 456.7 K on 1st cooling (5 K min^{-1}).

Table S3. Experimental and calculated q (=$4\pi \sin\theta/\lambda$ with 2θ and λ being scattering angle and wavelength of X-rays, respectively) for the Col$_h$ phase of B-MPB-22 at 456.7 K on 1st cooling (5 K min^{-1}) the SAXS pattern of which is given above in Figure S11.

Col$_h$ with a = 4.481±0.004 nm at 456.7 K on cooling				
(hk)	q_{obs} / nm^{-1}	q_{calc} / nm^{-1}	d_{obs} / nm	d_{calc} / nm
(10)	1.621	1.619	3.876	3.881
(11)	2.805	2.804	2.240	2.240
(20)	3.234	3.238	1.943	1.940

Table S4. Experimental and calculated q in the SAXS pattern for the Col_h phase of MB-MPB-22 at 422.9 K on 1st cooling (5 K min^{-1}) the SAXS pattern of which is given in Figure S9d.

Col_h with a = 4.089±0.001 nm at 422.9 K on cooling				
(hk)	q_{obs} / nm^{-1}	q_{calc} / nm^{-1}	d_{obs} / nm	d_{calc} / nm
(10)	1.774	1.775	3.542	3.541
(11)	3.074	3.074	2.044	2.044
(20)	3.549	3.549	1.770	1.770

Table S5. Experimental and calculated q in the SAXS pattern for the Col_h phase of MB-MPB-22 at 428.8 K on 2nd heating (5 K min^{-1}) the SAXS pattern of which is given in Figure S9d.

Col_h with a = 4.110±0.001 nm at 428.8 K on heating				
(hk)	q_{obs} / nm^{-1}	q_{calc} / nm^{-1}	d_{obs} / nm	d_{calc} / nm
(10)	1.765	1.765	3.560	3.559
(11)	3.060	3.058	2.054	2.055
(20)	3.530	3.531	1.780	1.780

4. Molecular structure and electron density map for single molecules based on DFT calculations

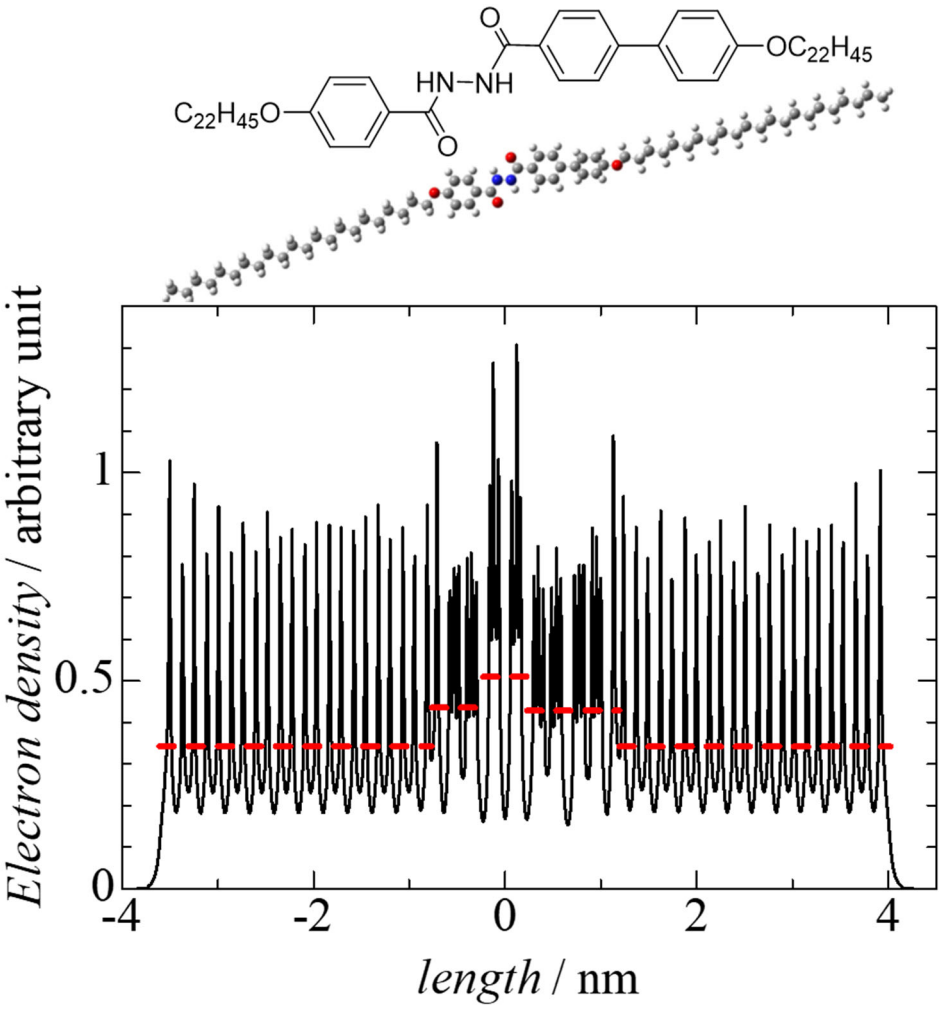

Figure S12. Molecular structure and electron density map obtained from the quantum chemical calculation for B-PB-22; the latter map is that integrated within a plane normal to the molecular long axis (solid curve) and its three-step approximation (dashed curve). Estimated molecular and core lengths are 7.42 and 1.86 nm, respectively.

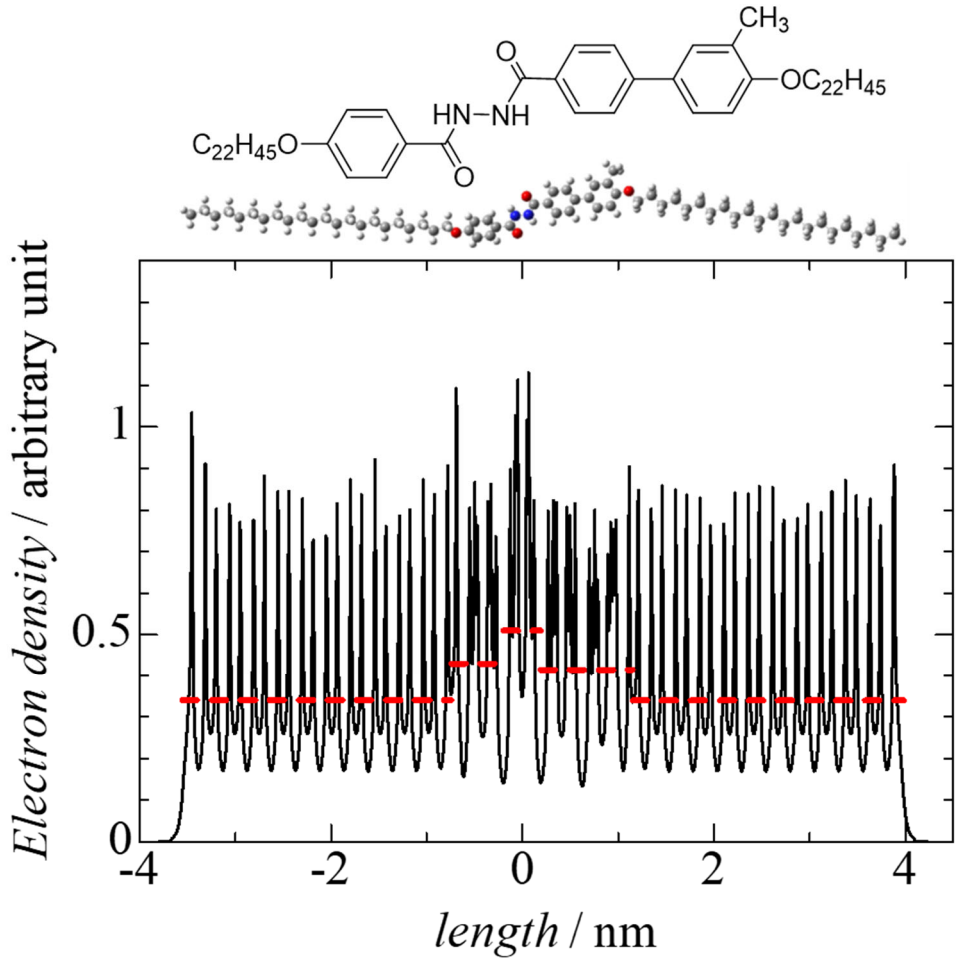

Figure S13. Molecular structure and electron density map obtained from the quantum chemical calculation for B-MPB-22; the latter map is that integrated within a plane normal to the molecular long axis (solid curve) and its three-step approximation (dashed curve). Estimated molecular and core lengths are 7.34 and 1.86 nm, respectively.

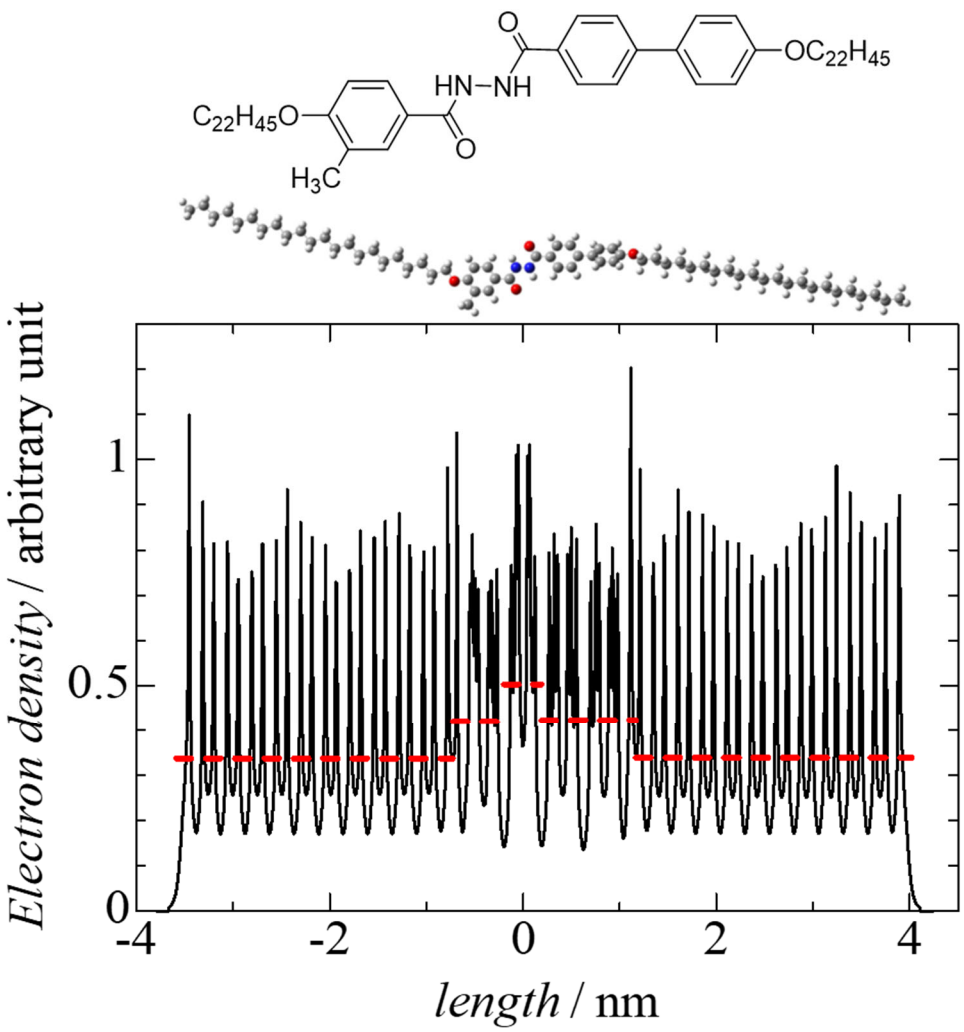

Figure S14. Molecular structure and electron density map obtained from the quantum chemical calculation for MB-PB-22; the latter map is that integrated within a plane normal to the molecular long axis (solid curve) and its three-step approximation (dashed curve). Estimated molecular and core lengths are 7.35 and 1.86 nm, respectively.

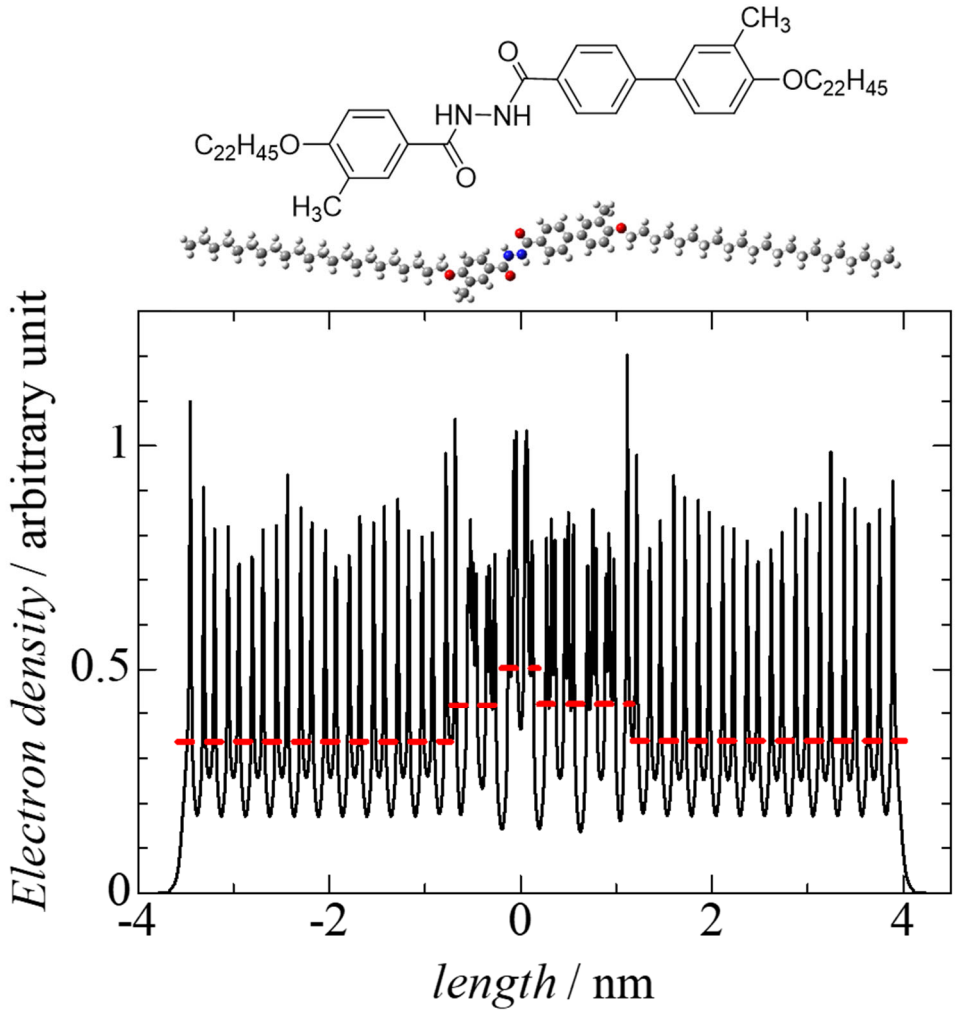

Figure S15. Molecular structure and electron density map obtained from the quantum chemical calculation for MB-MPB-22; the latter map is that integrated within a plane normal to the molecular long axis (solid curve) and its three-step approximation (dashed curve). Estimated molecular and core lengths are 7.33 and 1.86 nm, respectively.

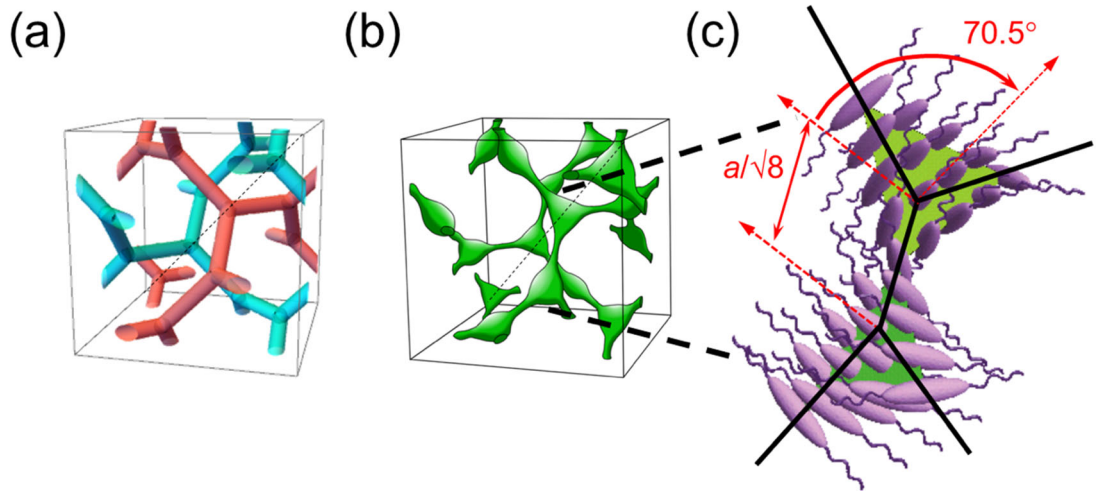

Figure S16. (a) Schematic representation of the network structure of $Ia\bar{3}d$ cubic phase. Two networks of red and light blue pipes joined 3-by-3 are enantiotropic with each other; (b) Triangular model representing high-density molecular cores regions; (c) schematic representation for helical molecular arrangement in the single-layered core assembly mode. In (a) and (b), thin broken lines are one of the body diagonals of the unit cell.

5. Electron density map based on MEM analyses

Table S6. SAXS data used for the MEM analyses of *Ia*3*d*-Cub phases (*hkl*, Miller index of respective diffraction plane; d_{obs} and d_{cal}, measured and best-fit *d*-spacings of diffraction peaks, respectively; $|F_{obs}|$ and F_{cal}, observed and calculated *F* values, normalized to $|F_{obs}$ (211)|, respectively; $\sigma(F_{cal})$, error). The 211 in the first column, for example, stands for (+2, +1, +1) and *F*(*hkl*) with other combinations of signs (to *h*, *k*, and *l*) may have an opposite sign.)

(a) BPB-22 at 448.3 K on heating

hkl	d_{obs} / nm	d_{cal} / nm [§]	$\|F_{obs}\|$	F_{cal}	$\sigma(F_{cal})$
211	4.34	4.34	1.000	-1.000	0.010
220	3.76	3.76	0.490	-0.496	0.004
321	2.84	2.84	0.018	-0.018	0.001
400	2.66	2.66	0.144	-0.149	0.003
420	2.38	2.38	0.102	0.103	0.001
332	2.27	2.27	0.144	-0.145	0.002
422	2.17	2.17	0.154	-0.156	0.002
431	2.08	2.09	0.087	-0.088	0.001
521	1.94	1.94	0.022	0.022	0.002
440	1.88	1.88	0.039	0.037	0.003

[§] a = 10.633±0.001 nm

(b) B-MPB-22 at 443.4 K on heating

hkl	d_{obs} / nm	d_{cal} / nm [§]	$\|F_{obs}\|$	F_{cal}	$\sigma(F_{cal})$
211	4.12	4.11	1.000	-1.000	0.008
220	3.57	3.56	0.579	-0.580	0.019
321	2.67	2.69	0.065	-0.054	0.034
400	2.51	2.52	0.113	-0.108	0.163
420	2.26	2.25	0.167	-0.139	0.037
332	2.15	2.15	0.273	0.208	0.044
422	2.05	2.06	0.243	0.118	0.062
431	1.98	1.97	0.086	0.079	0.030

[§] a = 10.07±0.01 nm

(c) MB-PB-22 at 425.9 K on heating

hkl	d_{obs} / nm	d_{cal} / nm [§]	$\|F_{obs}\|$	F_{cal}	$\sigma(F_{cal})$
211	4.01	4.02	1.000	-1.000	0.011
220	3.47	3.48	0.402	-0.402	0.010
321	2.63	2.63	0.006	0.006	0.001
400	2.46	2.46	0.141	-0.141	0.002
420	2.20	2.20	0.132	-0.131	0.002
332	2.10	2.10	0.151	-0.146	0.005
422	2.01	2.01	0.146	-0.128	0.006
431	1.93	1.93	0.070	0.067	0.005
521	1.80	1.80	0.012	0.012	0.002
440	1.74	1.74	0.028	0.028	0.003
541	1.52	1.52	0.018	0.017	0.001

[§] a = 9.843±0.003 nm

(d) MB-MPB-22 at 387.6 K on heating

hkl	d_{obs} / nm	d_{cal} / nm [§]	$\|F_{obs}\|$	F_{cal}	$\sigma(F_{cal})$
211	3.79	3.79	1.000	-1.000	0.023
220	3.28	3.28	0.474	-0.475	0.012
400	2.32	2.32	0.187	-0.185	0.009
420	2.08	2.08	0.181	0.136	0.013
332	1.98	1.98	0.213	0.195	0.012
422	1.90	1.90	0.164	-0.154	0.009
431	1.82	1.82	0.085	-0.085	0.004
521	1.69	1.70	0.007	0.007	0.001
440	1.64	1.64	0.029	-0.029	0.002
611/532	1.50	1.51	0.014	0.014	0.002
620	1.47	1.47	0.010	-0.010	0.003
631	1.36	1.37	0.003	0.003	0.001
444	1.34	1.34	0.018	-0.019	0.005
543	1.31	1.31	0.011	0.011	0.001
640	1.28	1.29	0.008	0.008	0.001

[§] a = 9.289±0.003 nm

(e) MB-MPB-22 at 338.4 K on heating

hkl	d_{obs} / nm	d_{cal} / nm [§]	$\|F_{obs}\|$	F_{cal}	$\sigma(F_{cal})$
211	3.75	3.75	1.000	-1.000	0.012
220	3.25	3.25	0.455	-0.456	0.009
400	2.30	2.30	0.189	-0.190	0.003
420	2.05	2.06	0.185	0.170	0.006
332	1.96	1.96	0.210	0.205	0.005
422	1.88	1.88	0.173	-0.165	0.005
431	1.80	1.80	0.086	-0.086	0.002
440	1.62	1.62	0.037	-0.037	0.002
611/532	1.49	1.49	0.011	0.011	0.001
631	1.36	1.36	0.004	-0.004	0.000
444	1.33	1.33	0.017	0.017	0.001
640	1.27	1.27	0.006	0.007	0.003

[§] a = 9.192±0.003 nm

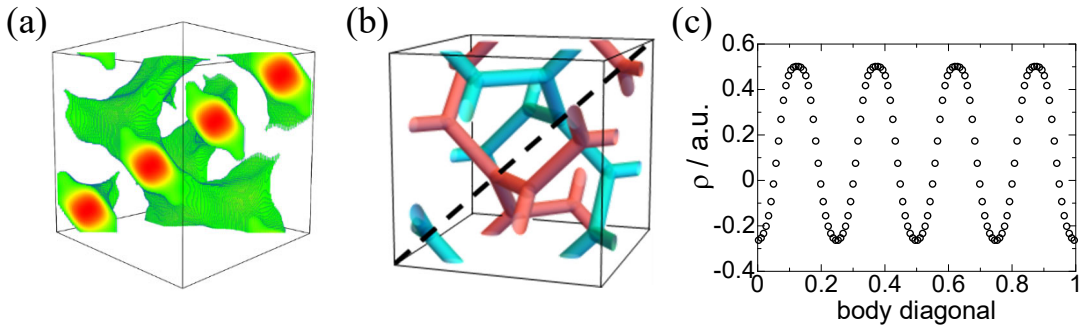

Figure S17. (a) Electron density map and (c) density profile as a function of the fraction along the body diagonal line of the unit cell of $Ia\bar{3}d$ cubic phase for MB-MPB-22 at 338.4 K (a = 9.192 nm) reconstructed by MEM analyses [green (medium) to red (high)]. The region with a lower density than the average is shown transparent. (b) Schematic representation of the network structure of $Ia\bar{3}d$ cubic phase. Two networks of red and light blue pipes joined 3-by-3 are enantiotropic with each other and the four 3-way junctions are aligned along the body diagonal line indicated by a broken line. The red regions in (a) correspond to the locations of the four 3-way junctions in (b), which are also the places of core assemblies because the high density region of the single molecules is the central dicarbonylhydrazine (–C=O–N-H–N-H–C=O–) linkages as revealed by Figures S12-S15.

6. IR

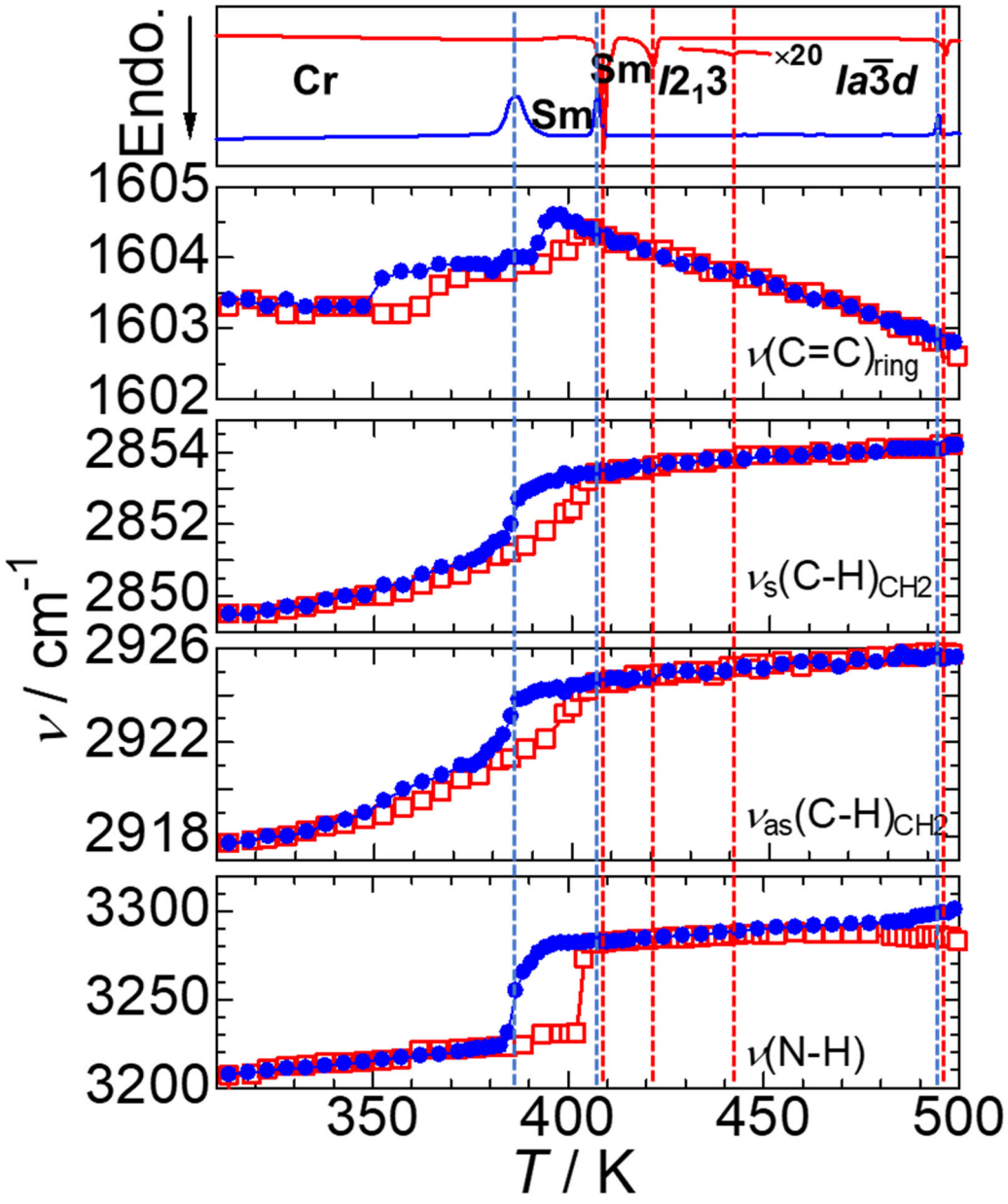

Figure S18. Four FT-IR band frequencies of $\nu(C=C)_{ring}$, $\nu_s(C\text{-}H)_{CH2}$, $\nu_{as}(C\text{-}H)_{CH2}$, and $\nu(N\text{-}H)$ of B-PB-22 as a function of temperature both on heating (□) and cooling (•), together with the corresponding DSC curves.

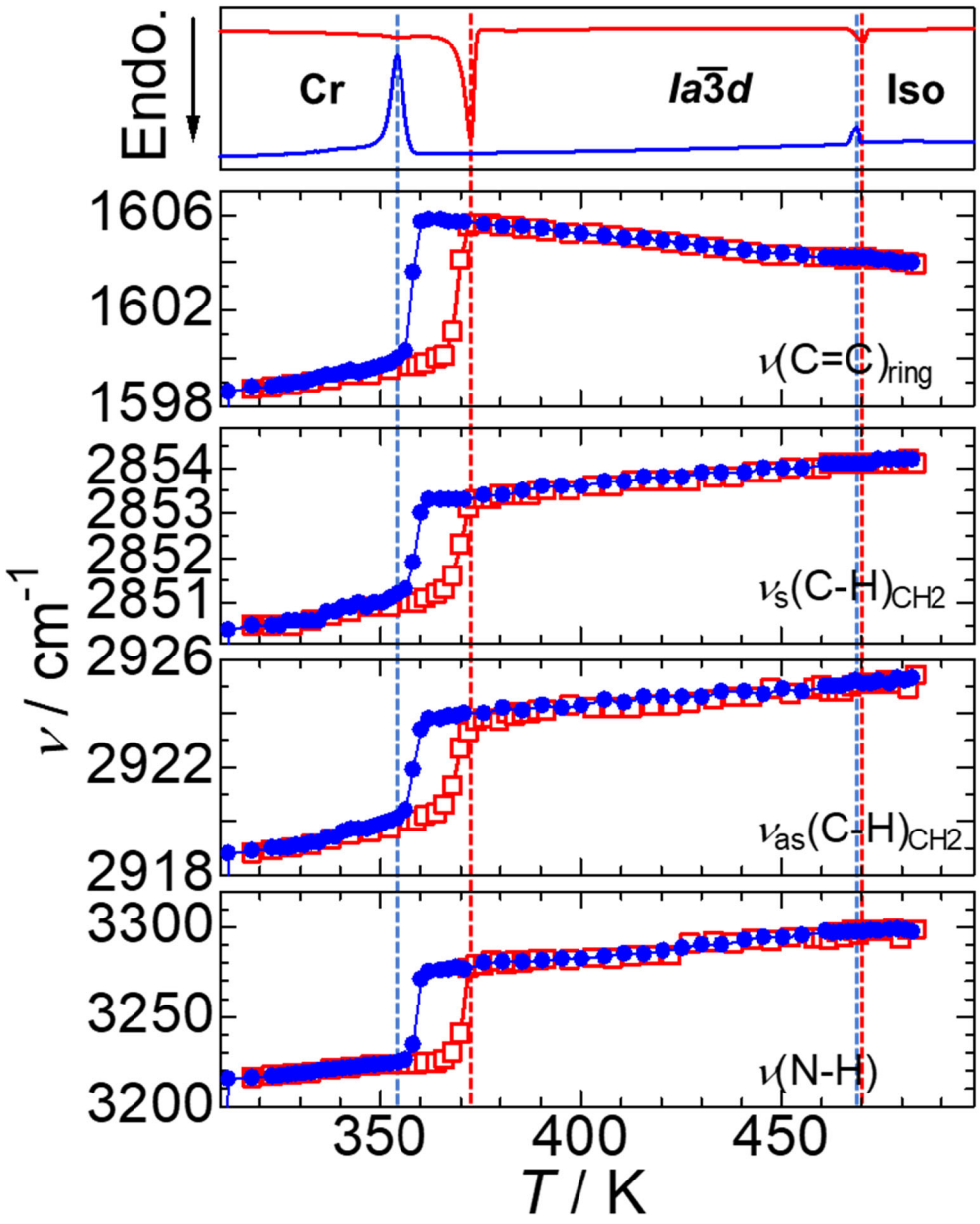

Figure S19. Four FT-IR band frequencies of $\nu(C=C)_{ring}$, $\nu_s(C\text{-}H)_{CH2}$, $\nu_{as}(C\text{-}H)_{CH2}$, and $\nu(N\text{-}H)$ of B-MPB-22 as a function of temperature both on heating (□) and cooling (•), together with the corresponding DSC curves.

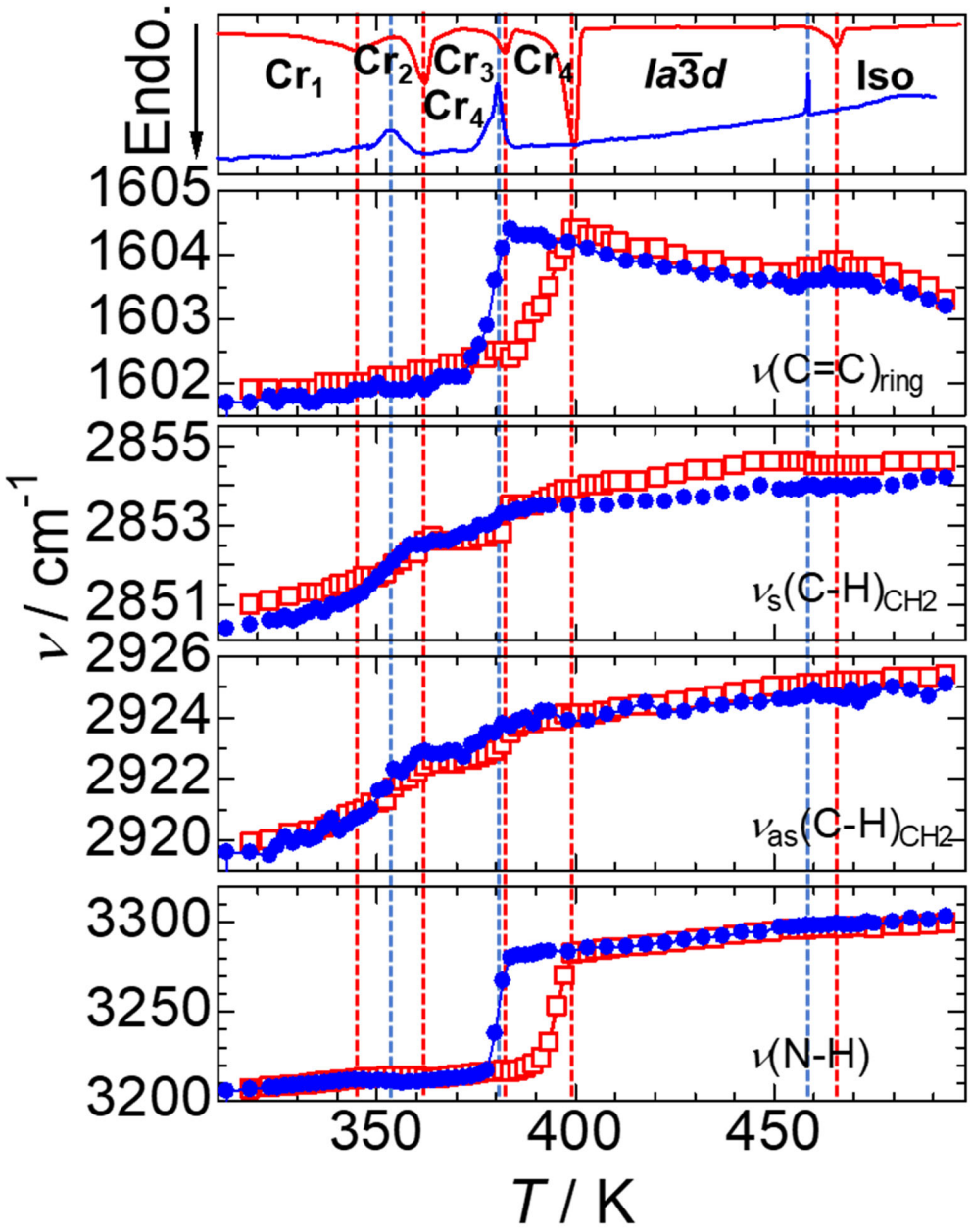

Figure S20. Four FT-IR band frequencies of $\nu(C{=}C)_{ring}$, $\nu_s(C\text{-}H)_{CH2}$, $\nu_{as}(C\text{-}H)_{CH2}$, and $\nu(N\text{-}H)$ of MB-PB-22 as a function of temperature both on heating (□) and cooling (•), together with the corresponding DSC curves.

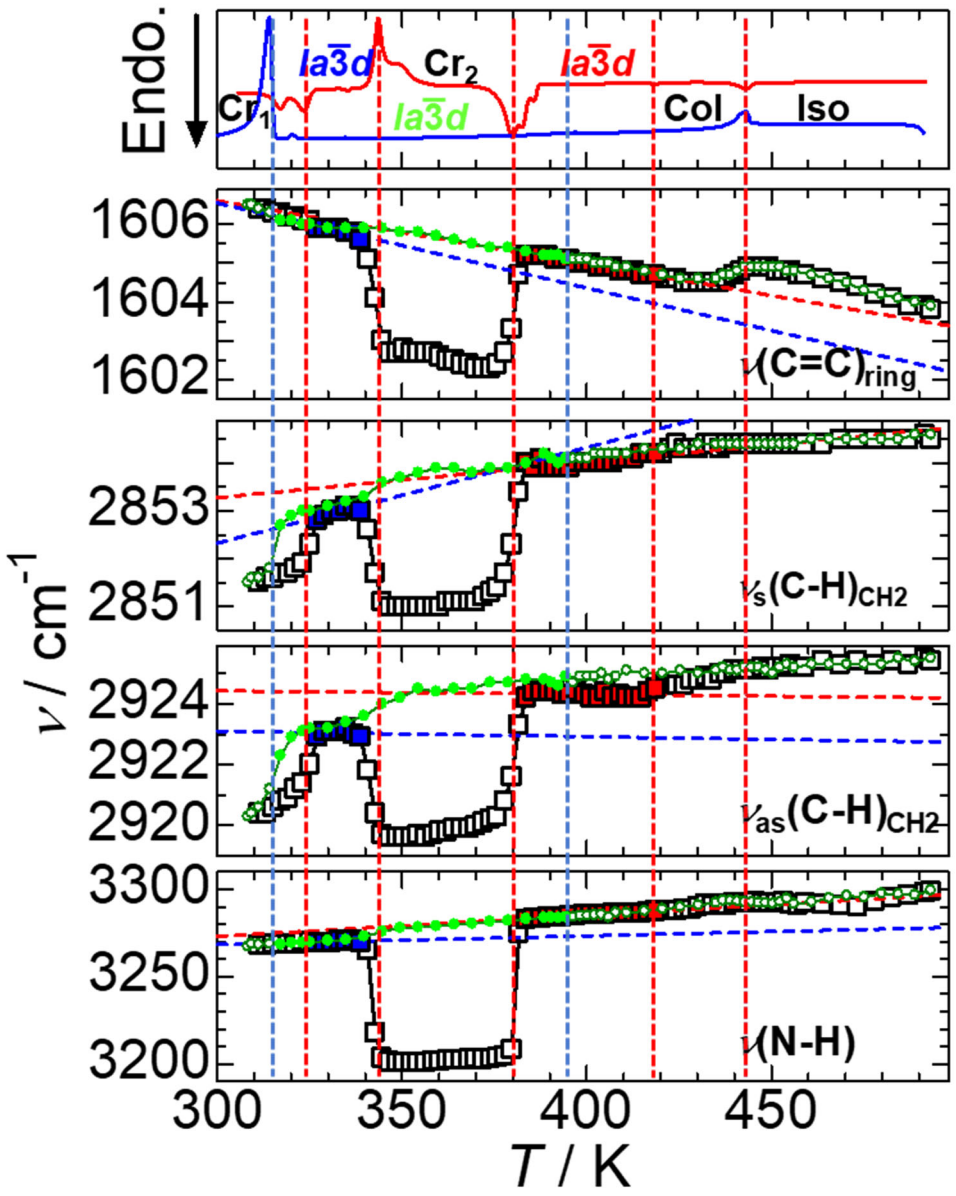

Figure S21. Four FT-IR band frequencies of $\nu(C=C)_{ring}$, $\nu_s(C\text{-}H)_{CH2}$, $\nu_{as}(C\text{-}H)_{CH2}$, and $\nu(N\text{-}H)$ of MB-MPB-22 as a function of temperature both on heating (red, blue, and open squares) and cooling (light green full and dark green open circles), together with the corresponding DSC curves.

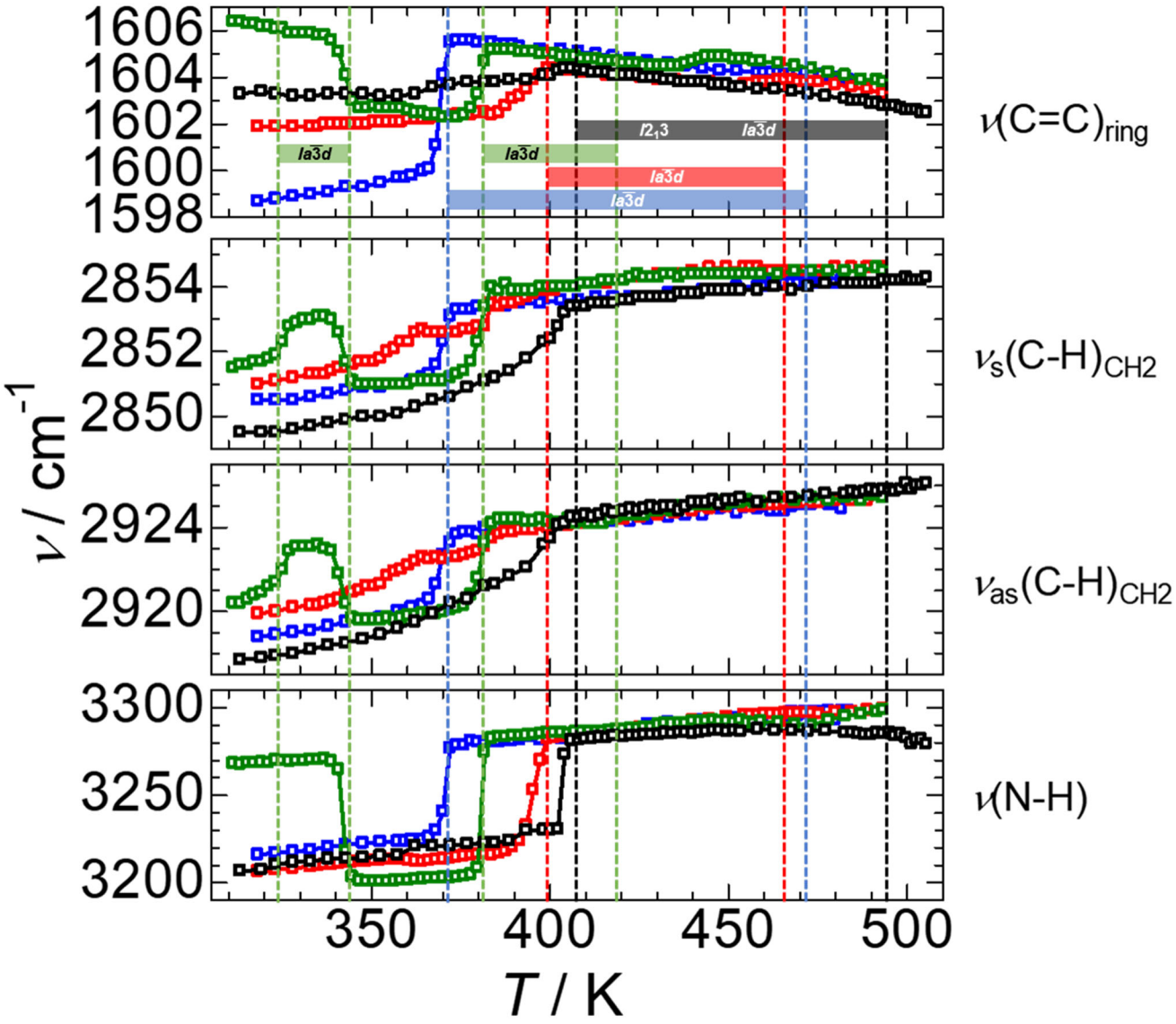

Figure S22. Four FT-IR Four FT-IR band frequencies of ν(C=C)$_{ring}$, ν_s(C-H)$_{CH2}$, ν_{as}(C-H)$_{CH2}$, and ν(N-H) of B-PB-22 (■), B-MPB-22 (■), MB-PB-22 (■), and MB-MPB-22 (■) as a function of temperature on heating.

7. Interaction energy calculation based on quantum chemical calculations and NCI analysis

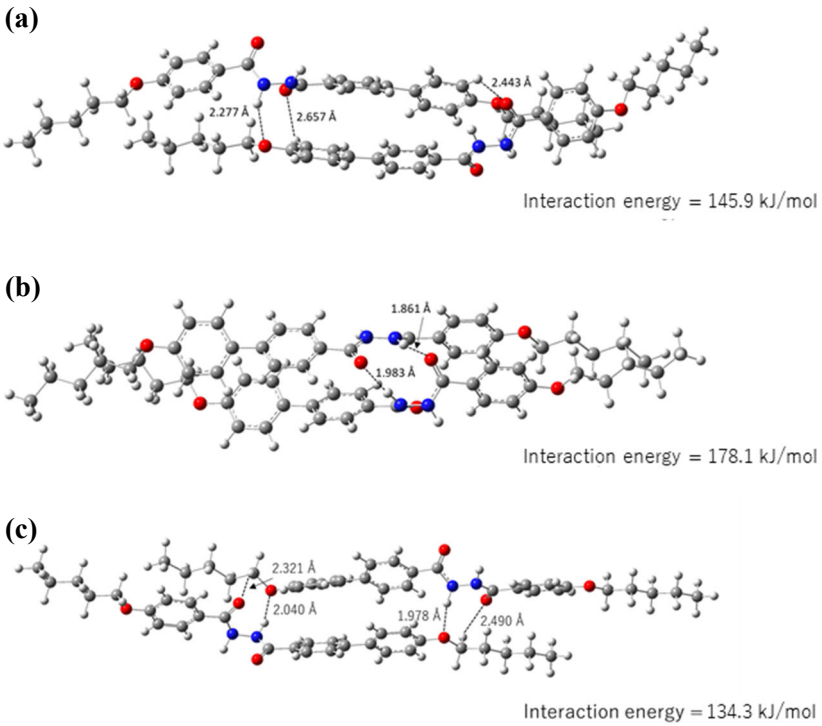

Figure S23. Three geometry-optimized dimeric pairs within the $Ia\bar{3}d$ networks assumed for B-PB-22 in Fig. 6 in the main text, together with the interaction energies of those pairs based on the B3LYP+GD3 theories with 6-31G** basis set.

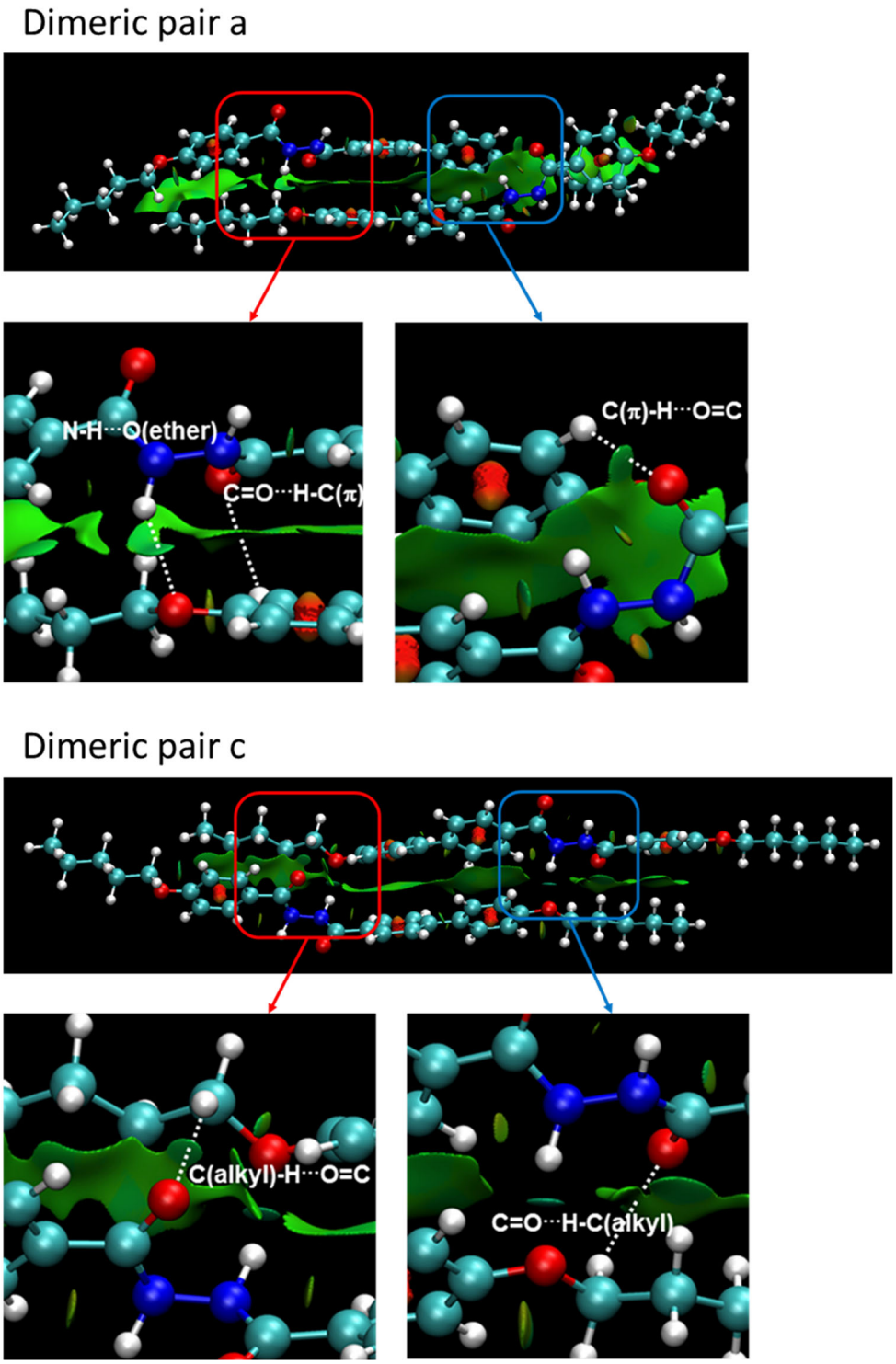

Figure S24. NCI analyses for the two dimeric pairs a and c given in Figure S23 assumed for the $Ia\bar{3}d$ networks of B-PB-22, where red (seen within benzene rings) represents repulsive interaction whereas green represents weak interactions such as van der Waals interactions; the existence of intermolecular π-π interactions between two neighboring core potions, and weak hydrogen bonding interactions such as -N-H···O(ether)<, -C=O···H-C(π)- and –C=O···H-C(alkyl)- are visualized.

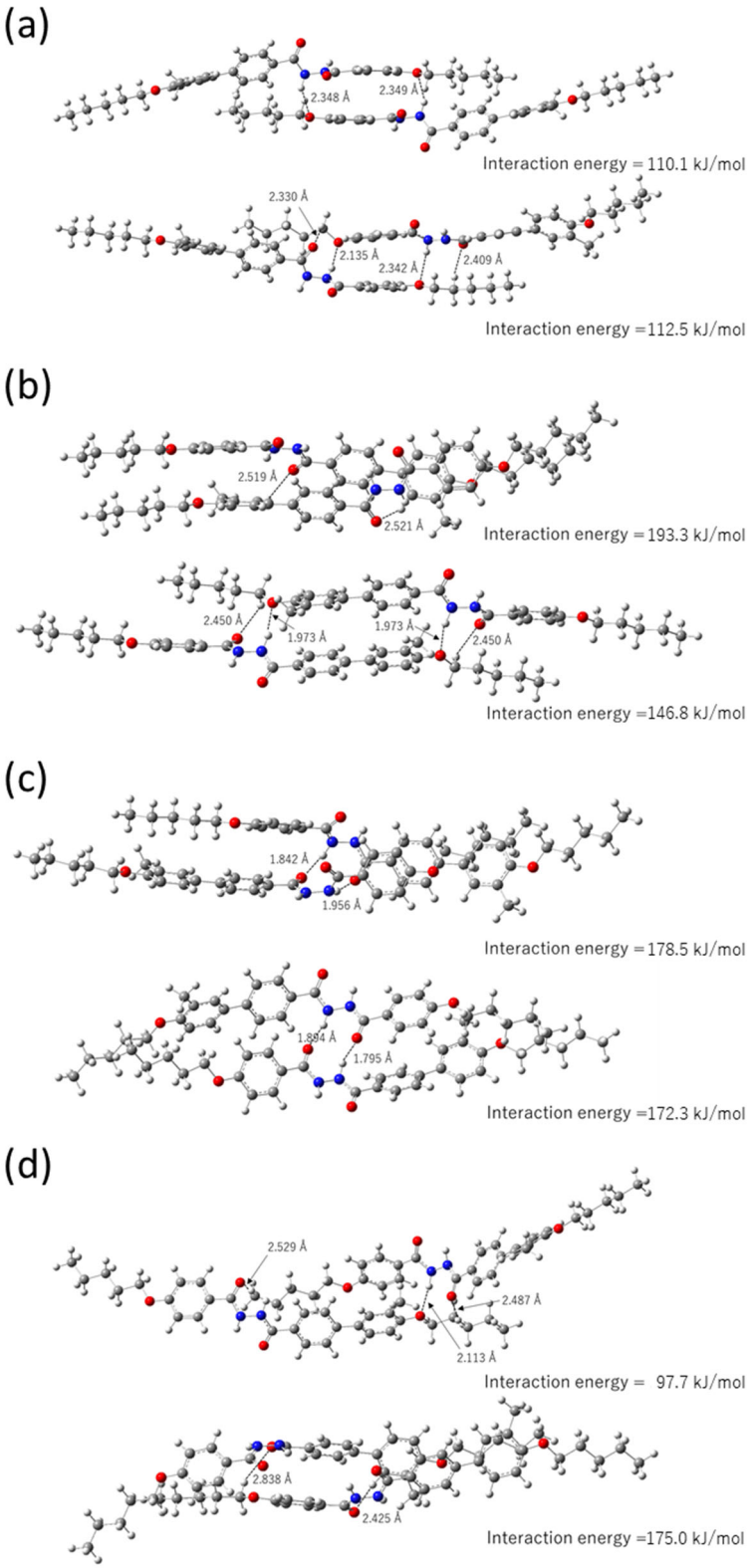

Figure S25. Geometry-optimized dimeric pairs within the four molecular arrangements of the $Ia\bar{3}d$ network assumed for B-MPB-22 in Fig. 7 in the main text, together with the interaction energies of those pairs based on the B3LYP+GD3 theories with 6-31G** basis set.

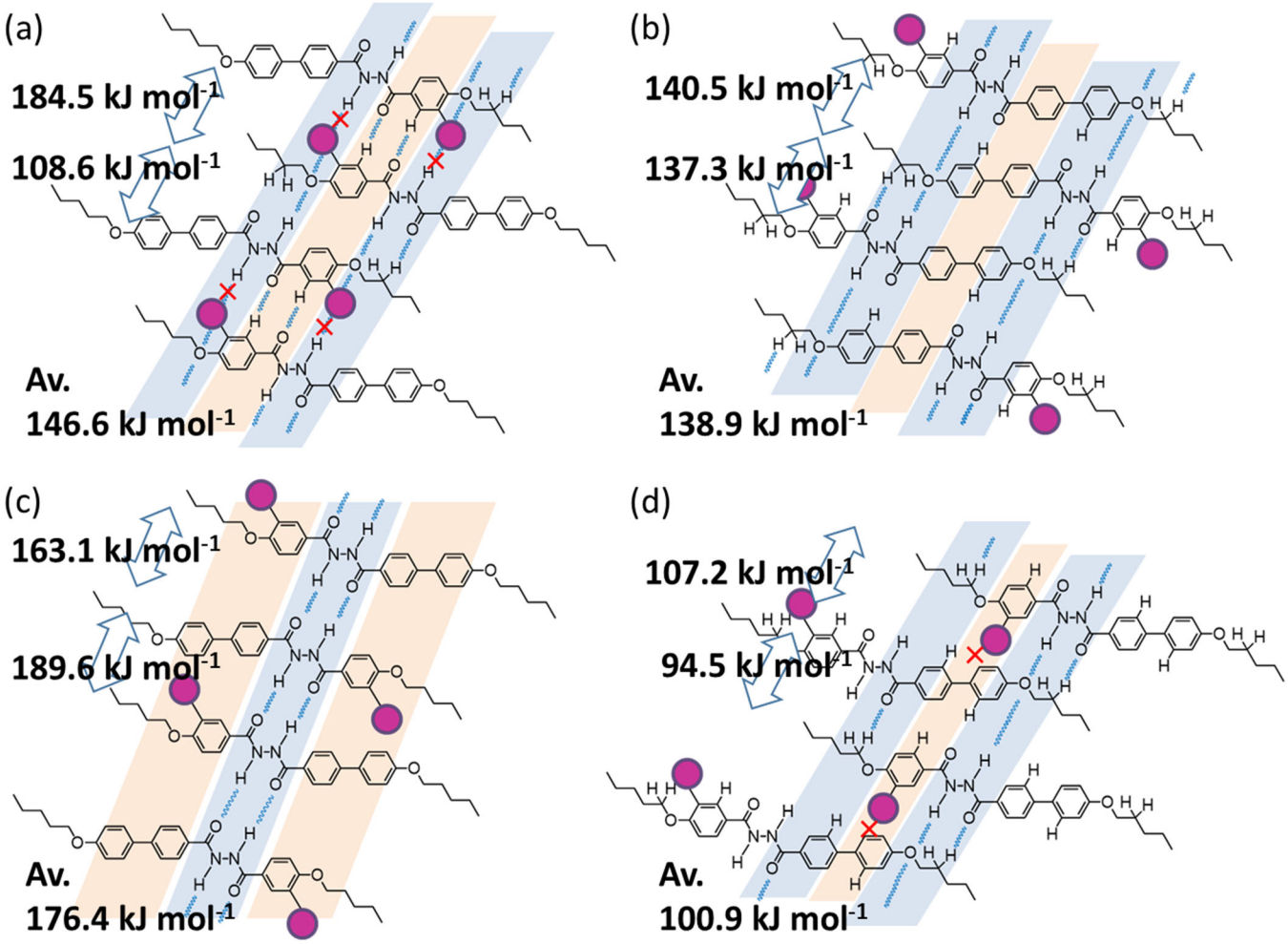

Figure S26. Schematic molecular arrangements for MB-PB-22, together with interaction energies of dimeric pairs in each arrangement as evaluated using B3LYP+GD3 theories with 6-31G** basis set. Dark red circles represent methyl side-group in the phenyl rings. In (a), the large interaction energy (184.5 kJ mol^{-1}) between neighboring molecules probably comes from the strong –N-H···O=C– interaction between the two outward-directed C=O and H-N groups of different molecules (see Figure S27a), which is due to the (actually unrealistic but technically inevitable) assumption of no neighboring molecules above and below the dimeric pair and different from the arrangement represented above.

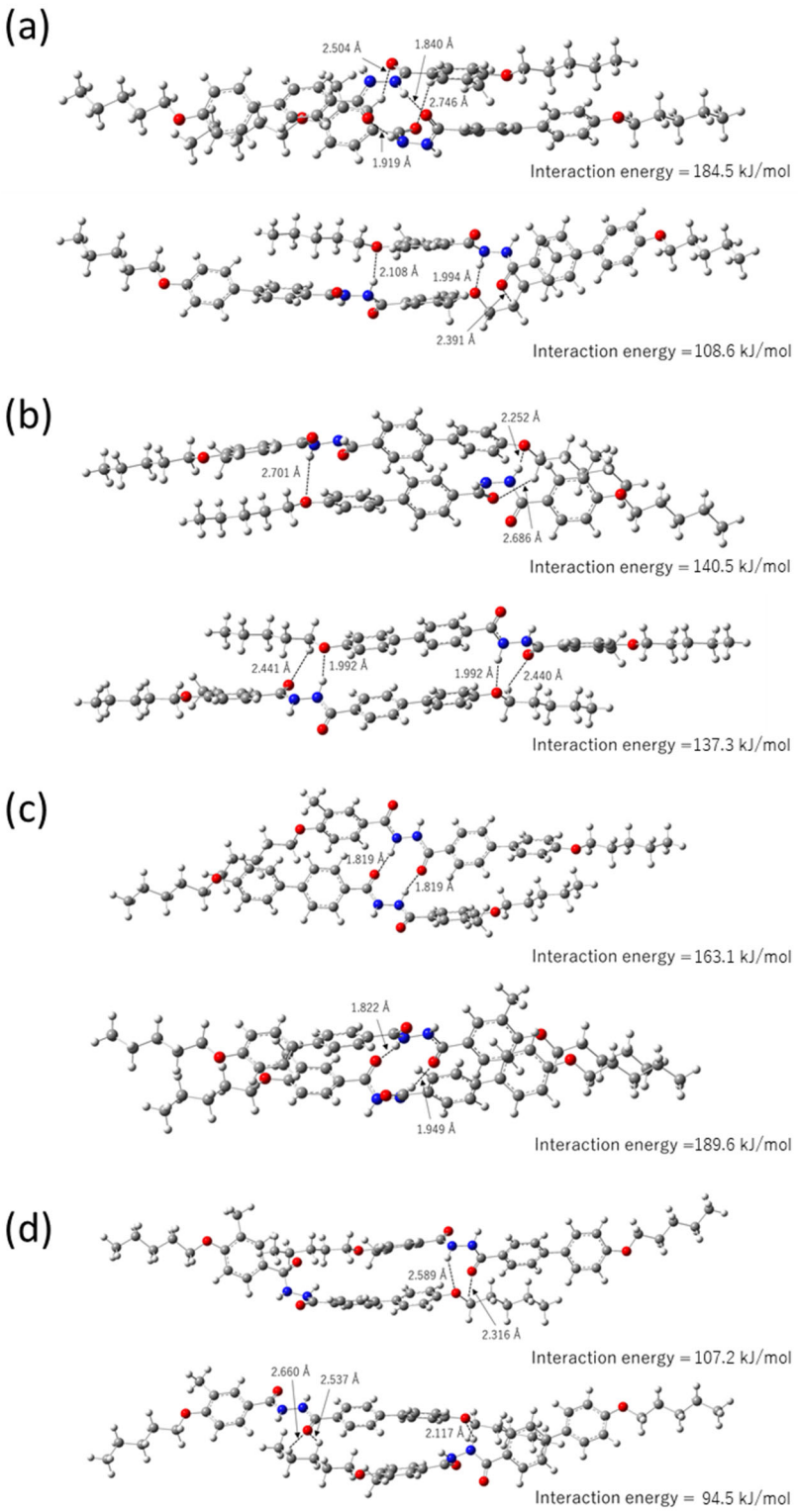

Figure S27. Geometry-optimized dimeric pairs within the four molecular arrangements of the $Ia\bar{3}d$ network assumed for MB-PB-22 in Figure S26 above, together with the interaction energies of those pairs based on the B3LYP+GD3 theories with 6-31G** basis set.

8. Synthetic details for B-MPB-22, MB-PB-22, and MB-MPB-22

8.1. Synthesis of B-MPB-22

a. Preparation of Ethyl 4-(4′-hydroxy-3′-methylphenyl)benzoate:[S2] 4-bromo-2-methylphenol (1.76 g, 9.39 mmol) and 4-(ethoxycarbonyl)phenylboronic acid (2.91 g, 15.0 mmol) were mixed with an aqueous solution (35 mL) of K_2CO_3 (2.12 g, 20.0 mmol), to which an *N,N*-dimethylformamide (DMF) (30 mL) solution of palladium (II) acetate (0.0233 g, 0.104 mmol) was added. The resulting solution was refluxed at 35 °C for 23 h. After cooled, the solution was acidified with sulfuric acid (2 mL). Chloroform ($CHCl_3$) (50 mL) was added and the organic layer was separated. This procedure was repeated four times. The solvent was removed by a rotary evaporator. The obtained product was further purified by chromatography (eluent: *n*-hexane : ethyl acetate = 4 : 1 (*v*/*v*)) to give a white solid. The final product was dried at 50 °C under vacuum for 11 h to give 1.57 g (6.11 mmol, 65 %).

^{1}H NMR (400 MHz, $CDCl_3$, r.t.): δ 8.07 (d, J = 8.4 Hz, 2H, Ar−H), 7.60 (d, J = 8.4 Hz, 2H, Ar−H), 7.41 (s, 1H, Ar−H), 7.36 (d, J = 8.4 Hz, 1H, Ar−H), 6.86 (d, J = 8.4 Hz, 2H, Ar−H), 4.88 (s, 1H, Ar−OH), 4.38 (q, J = 7.2 Hz, 2H, $COOCH_2CH_3$), 2.33 (s, 3H, Ar-CH_3), 1.41 (t, J = 7.2 Hz, 3H, $COOCH_2CH_3$).

b. Preparation of Ethyl 4-(4′-n-dodecyloxy-3′-methylphenyl)benzoate:[S1] Ethyl 4-(4′-hydroxy-3′-methylphenyl)benzoate (1.57 g, 6.11 mmol), 1-bromo-*n*-dodecane (2.85 g, 7.33 mmol), and K_2CO_3 (1.69 g, 12.2 mmol) were dissolved in acetone (60 mL), and refluxed at 60 °C for 38 h. After cooled, $CHCl_3$ (50 mL) was added and the organic layer was separated. This procedure was repeated three times. After drying with $MgSO_4$, the solvent was removed by evaporation. The obtained product was further purified by chromatography (eluent: *n*-hexane : ethyl acetate = 30 : 1 (*v*/*v*)) to give a white solid. The final product was dried at 60 °C in vacuum for 24 h to give 2.00 g (3.55 mmol, 58 %).

^{1}H NMR (400 MHz, $CDCl_3$, r.t.): δ 8.07 (d, J = 8.0 Hz, 2H, Ar−H), 7.61 (d, J = 8.4 Hz, 2H, Ar−H), 7.42 (s, 1H, Ar−H), 7.41 (s, 1H, Ar−H), 6.89 (d, J = 9.2 Hz, 1H, Ar−H), 4.39 (q, J = 7.1 Hz, 2H, $COOCH_2CH_3$), 4.01 (t, J = 6.4 Hz, 2H, OCH_2), 2.29 (s, 3H, Ar-CH_3), 1.87-1.75 (m, 2H, OCH_2CH_2), 1.49 (quin, J = 7.6 Hz, 2H, $OCH_2CH_2CH_2$), 1.41 (t, J = 7.0 Hz, 3H, $COOCH_2CH_3$), 1.34-1.16 (m, 36H, $OCH_2CH_2CH_2(CH_2)_{18}$), 0.88 (t, J = 7.0 Hz, 3H, CH_3).

c. Preparation of 4-(4′-n-dodecyloxy-3′-methylphenyl)benzoic acid:[S1] Ethyl 4-(4′-*n*-dodecyloxy-3′-methylphenyl)benzoate (2.00 g, 3.55 mmol) was dissolved in ethanol (80

mL), to which aqueous solution (20 mL) of NaOH (2.21 g, 55.2 mmol) was slowly added and 1he resulting mixture was refluxed at 80 °C for 21 h. After cooled to room temperature, the white precipitate was collected and then dissolved in toluene while heated, to which 12N HCl (8 mL) was added dropwise while stirred at room temperature. The solvent was removed by a rotary evaporator. The obtained white solid was recrystallized from toluene. The final white crystalline solid was dried under vacuum at 80 °C for 24 h to give 1.62 g (3.02 mmol, 85 %).

^{1}H NMR (400 MHz, $CDCl_3$, r.t.): δ 8.10 (d, J = 8.4 Hz, 2H, Ar−H), 7.64 (d, J = 8.0 Hz, 2H, Ar−H), 7.42 (s, 1H, Ar−H), 7.41 (s, 1H, Ar−H), 6.89 (d, J = 9.2 Hz, 1H, Ar−H), 4.02 (t, J = 6.4 Hz, 2H, OCH_2), 2.29 (s, 3H, Ar-CH_3), 1.83 (quin, J = 6.9 Hz, 2H, OCH_2CH_2), 1.55-1.40 (m, 2H, $O\,CH_2CH_2CH_2$), 1.4-1.2 (m, 36H, $OCH_2CH_2CH_2(CH_2)_{18}$), 0.88 (t, J = 7.0 Hz, 3H, CH_3).

d. Preparation of N-(4-n-dodecyloxybenzoyl)-N′-(4-(4′-n-dodecyloxy-3′-methylphenyl)benzoyl)-hydrazine (B-MPB-22):[S3] 4-(4′-*n*-dodecyloxy-3′-methylphenyl)benzoic acid (0.50 g, 0.937 mmol) was dissolved into dry toluene (20 mL), to which thionyl chloride (0.08 mL, 1.11 mmol) and three drops of DMF were added and refluxed at 80 °C for 3 h under N_2 atmosphere. After cooled to room temperature, the remaining thionyl chloride and the solvent were removed thoroughly under a reduced pressure to give the acid chloride, to which 20 mL of dry toluene was added to give a solution. 4-*n*-dodecyloxybenzoylhydrazide (0.47 g, 1.03 mmol) and a drop of *N*,*N*-diisopropylethylamine (DIPEA) were dissolved in 20 mL of dry toluene, to which the above solution was slowly added dropwise for 10 min while heating and stirring. The solution was further refluxed at 80 °C for 17 h. After cooling to room temperature, a while precipitate was collected. The product was washed with hot water, and recrystallized from acetone, THF, and toluene, and dried at 60 °C under vacuum for 18 h, yielding 0.282 g (0.287 mmol, 31 %).

^{1}H NMR (400 MHz, $CDCl_3$): δ 9.13 (d, J = 6.8 Hz, 1H, N−H), 9.02 (d, J = 6.8 Hz, 1H, N−H), 7.89 (d, J = 8.8 Hz, 2H, Ar−H), 7.83 (d, J = 9.2 Hz, 2H), 7.65 (d, J = 8.4 Hz, 2H, Ar−H), 7.41 (s, 1H, Ar-H), 7.40 (s, 1H, Ar−H), 6.95 (d, J = 9.2 Hz, 2H, Ar−H), 6.89 (d, J = 9.2 Hz, 1H, Ar−H), 4.02 (t, J = 6.6 Hz, 4H, OCH_2), 2.29 (s, 3H, Ar-CH_3), 1.87-1.75 (m, 4H, OCH_2CH_2), 1.55-1.42 (m, 4H, $OCH_2CH_2CH_2$), 1.4-1.2 (m, 72H, $OCH_2CH_2CH_2(CH_2)_{18}$), 0.88 (t, J = 7.0 Hz, 6H, CH_3).

Elemental Anal. Calcd for $C_{65}H_{106}N_2O_4$: C, 79.70; H, 10.91; N, 2.86. Found: C, 79.38; H, 11.04; N, 2.99 %.

8.2. Synthesis of MB-PB-22

a. Preparation of Ethyl 4-hydroxy-3-methylbenzoate: 4-hydroxy-3-methylbenzoic acid (2.00 g, 13.1 mmol) was dissolved in ethanol (35 mL), to which sulfuric acid (0.30 mL, 5.6 mmol) was added. The resulting solution was refluxed at 80 °C for 45.5 h. After cooled, the solvent was removed by a rotary evaporator. Diethyl ether (20 mL) was added and the organic layer was separated. This procedure was repeated four times. The solvent was removed by a rotary evaporator. The obtained product was further purified by chromatography (eluent: *n*-hexane : ethyl acetate = 4 : 1 (*v*/*v*)) to give a white solid. The final product was dried at 60 °C under vacuum for 17 h to give 1.81 g (10.0 mmol, 76.3 %).
^{1}H NMR (400 MHz, $CDCl_3$, r.t.): δ 7.84 (s, 1H, Ar-H), 7.80 (d-d, J_1 = 8.4 Hz, J_2 = 2.4 Hz, 1H, Ar−H), 6.79 (d, J = 8.0 Hz, 1H, Ar−H), 5.35 (s, 1H, Ar−OH), 4.34 (q, J = 7.2 Hz, 2H, $COOCH_2CH_3$), 2.28 (s, 3H, Ar-CH_3), 1.38 (t, J = 7.2 Hz, 3H, $COOCH_2CH_3$).

b. Preparation of Ethyl 4-n-dodecyloxy-3-methylbenzoate:[S1] Ethyl 4-hydroxy-3-methylbenzoate (1.79 g, 9.95 mmol), 1-bromo-*n*-dodecane (4.67 g, 12.0 mmol), and K_2CO_3 (2.08 g, 15.0 mmol) were dissolved in dry acetone (40 mL), and refluxed at 60 °C for 24 h. After cooled, $CHCl_3$ (45 mL) was added and the organic layer was separated. This procedure was repeated four times. After drying with $MgSO_4$, the solvent was removed by evaporation. The obtained product was further purified by chromatography (eluent: *n*-hexane : ethyl acetate = 30 : 1 (*v*/*v*)) to give a white solid. The final product was dried at 60 °C in vacuum for 24 h to give 3.75 g (6.64 mmol, 67 %).
^{1}H NMR (400 MHz, $CDCl_3$, r.t.): δ 7.86 (d, J = 8.8 Hz, 1H, Ar−H), 7.82 (d, J = 1.6 Hz, 1H, Ar−H), 6.80 (d, J = 8.0 Hz, 1H, Ar−H), 4.34 (q, J = 7.2 Hz, 2H, $COOCH_2CH_3$), 4.01 (t, J = 6.4 Hz, 2H, OCH_2), 2.24 (s, 3H, Ar-CH_3), 1.81 (quin, J = 9.2 Hz, 2H, OCH_2CH_2), 1.48 (quin, J = 9.2 Hz, 2H, $OCH_2CH_2CH_2$), 1.38 (t, J = 7.2 Hz, 3H, $COOCH_2CH_3$), 1.35-1.19 (m, 36H, $OCH_2CH_2CH_2(CH_2)_{18}$), 0.88 (t, J = 7.0 Hz, 3H, CH_3).

c. Preparation of 4-n-dodecyloxy-3-methylbenzhydrazide:[S3] Hydrazine monohydrate (6.3 mL, 130 mmol) was dissolved in dry ethanol (20 mL) that was degassed by N_2 gas bubbling prior to use, to which ethyl 4-*n*-dodecyloxy-3-methylbenzoate (3.75 g, 6.64 mmol) was added and refluxed at 80 °C under N_2 atmosphere for 44 h. After cooled to room temperature, the solvent was removed by a rotary evaporator. The product was dried in vacuum at 60 °C for 20 h to give a white solid (0.75 g, 1.59 mmol, 24%).
^{1}H NMR (400 MHz, $CDCl_3$): δ 7.56 (s, 1H, Ar-H), 7.55 (s, 1H, Ar-H), 7.23 (s, 1H, $NHNH_2$), 6.82 (d, J = 8.0 Hz, 1H, Ar-H), 4.02 (s, 2H, $NHNH_2$), 4.00 (t, J = 6.6 Hz, 2H, OCH_2), 2.24 (s, 3H, Ar-CH_3), 1.81 (quin, J = 7.0 Hz, 2H, OCH_2CH_2), 1.5-1.4 (m, 2H,

*OCH₂CH₂*CH₂), 1.4-1.2 (m, 18H, *OCH₂CH₂*(CH₂)₉), 0.88 (t, *J* = 7.0 Hz, 3H, CH₃).

d. Preparation of N-(4-n-dodecyloxy-3-methylbenzoyl)-N′-(4-(4′-n-dodecyloxyphenyl)benzoyl)-hydrazine (MB-PB-22):[S3] 4-*n*-dodecyloxybenzoic acid (0.84 g, 1.60 mmol) was dissolved in dry toluene (20 mL), to which thionyl chloride (0.13 mL, 1.80 mmol) and three drops of DMF were added and refluxed at 80 °C for 5 h under N_2 atmosphere. After cooled to room temperature, the remaining thionyl chloride and solvent were removed thoroughly under a reduced pressure to give the acid chloride, to which 20 mL of dry toluene was added to give a solution. 4-*n*-dodecyloxy-3-methylbenzoylhydrazide (0.75 g, 1.59 mmol) and DIPEA (0.15 mL, 1.76 mmol) were dissolved in 20 mL of dry toluene, to which the above solution was slowly added dropwise for 7 min while stirring. The solution was further refluxed at 80 °C for 14 h. After cooling to room temperature, a white precipitate was collected. The product was washed with hot water, and recrystallized from THF once and toluene three times, and dried at 60 °C under vacuum for 18 h, yielding 0.793 g (0.810 mmol, 51 %).

^{1}H NMR (400 MHz, $CDCl_3$): δ 9.19 (d, *J* = 6.0 Hz, 1H, N−H), 9.04 (d, *J* = 6.4 Hz, 1H, N−H), 7.90 (d, *J* = 8.8 Hz, 2H, Ar−H), 7.70 (d, *J* = 8.8 Hz, 1H), 7.67 (s, 1H, Ar-H), 7.65 (d, *J* = 8.0 Hz, 2H, Ar−H), 7.54 (d, *J* = 8.4 Hz, 2H, Ar−H), 6.98 (d, *J* = 8.8 Hz, 2H, Ar−H), 6.85 (d, *J* = 8.4 Hz, 1H, Ar−H), 4.02 (q, *J* = 6.3 Hz, 4H, OCH_2), 2.26 (s, 3H, Ar-CH_3), 1.82 (six, *J* = 7.0 Hz, 4H, *OCH₂*CH₂), 1.56-1.42 (m, 4H, *OCH₂CH₂*CH₂), 1.42-1.22 (m, 72H, *OCH₂CH₂CH₂*(CH₂)₁₈), 0.88 (t, *J* = 7.0 Hz, 6H, CH_3).

Elemental Anal. Calcd for $C_{65}H_{106}N_2O_4$: C, 79.70; H, 10.91; N, 2.86. Found: C, 79.42; H, 10.62; N, 2.97 %.

8.3. Synthesis of MB-MPB-22

a. Preparation of Ethyl 4-hydroxy-3-methylbenzoate: 4-hydroxy-3-methylbenzoic acid (2.00 g, 13.2 mmol) was dissolved in ethanol (50 mL), to which sulfuric acid (0.80 mL, 15 mmol) was added. The resulting solution was refluxed at 80 °C for 20 h. After cooled, the solvent was removed by a rotary evaporator, and the remaining solution was neutralized with $NaHCO_3$ (0.60 g, 7.1 mmol). Ethyl acetate (30 mL) was added and the organic layer was separated. This procedure was repeated five times. After that, the solvent was removed by a rotary evaporator. The obtained product was further purified by chromatography (eluent: *n*-hexane : ethyl acetate = 3 : 1 (*v*/*v*)) to give a white solid. The final product was dried at 60 °C under vacuum for 21 h to give 2.21 g (12.2 mmol, 93 %).

^{1}H NMR (400 MHz, $CDCl_3$, r.t.): δ 7.84 (s, 1H, Ar-H), 7.80 (d, *J* = 8.6 Hz, 1H, Ar−H),

6.79 (d, J = 8.4 Hz, 1H, Ar−H), 5.37 (s, 1H, Ar−OH), 4.34 (q, J = 7.2 Hz, 2H, $COOCH_2CH_3$), 2.28 (s, 3H, Ar-CH_3), 1.38 (t, J = 7.0 Hz, 3H, $COOCH_2CH_3$).

b. Preparation of Ethyl 4-n-dodecyloxy-3-methylbenzoate:[S1] Ethyl 4-hydroxy-3-methylbenzoate (2.05 g, 11.4 mmol), 1-bromo-*n*-dodecane (4.89 g, 12.6 mmol), and K_2CO_3 (2.37 g, 17.1 mmol) were dissolved in dry acetone (50 mL). After being bubbled with N_2 gas for 30 min, the solution was refluxed at 80 °C for 25 h. After cooled, the solvent was removed by a rotary evaporator. $CHCl_3$ (60 mL) was added and the organic layer was separated. This procedure was repeated three times. The solvent was removed by a rotary evaporator. The obtained product was further purified by chromatography (eluent: *n*-hexane : ethyl acetate = 30 : 1 (*v*/*v*)) to give a white solid. The final product was dried at 60 °C in vacuum for 16 h to give 4.44 g (9.08 mmol, 80 %).

^{1}H NMR (400 MHz, $CDCl_3$, r.t.): δ 7.86 (d-d, J_1 = 8.8 Hz, J_2 = 2.4 Hz, 1H, Ar−H), 7.82 (d, J = 1.6 Hz, 1H, Ar−H), 6.80 (d, J = 8.0 Hz, 1H, Ar−H), 4.34 (q, J = 7.1 Hz, 2H, $COOCH_2CH_3$), 4.01 (t, J = 6.4 Hz, 2H, OCH_2), 2.24 (s, 3H, Ar-CH_3), 1.81 (quin, J = 7.0 Hz, 2H, OCH_2CH_2), 1.48 (quin, J = 7.6 Hz, 2H, $OCH_2CH_2CH_2$), 1.38 (t, J = 7.0 Hz, 3H, $COOCH_2CH_3$), 1.34-1.20 (m, 36H, $OCH_2CH_2CH_2(CH_2)_{18}$), 0.88 (t, J = 7.0 Hz, 3H, CH_3).

c. Preparation of 4-n-dodecyloxy-3-methylbenzhydrazide:[S3] Hydrazine monohydrate (5.4 mL, 111 mmol) was dissolved in dry ethanol (30 mL) that was degassed by N_2 gas bubbling for 1.5 h prior to use, to which ethyl 4-*n*-dodecyloxy-3-methylbenzoate (0.90 g, 1.84 mmol) was added and refluxed at 90 °C under N_2 atmosphere for 21 h. After cooled to room temperature, the solvent was removed by a rotary evaporator. The product was dried in vacuum at 60 °C for 7 h to give a white solid (0.57 g, 1.19 mmol, 65%).

^{1}H NMR (400 MHz, $CDCl_3$): δ 7.55 (d, J = 8.0 Hz, 1H, Ar-H), 7.54 (s, 1H, Ar-H), 7.21 (s, 1H, $NHNH_2$), 6.81 (d-d, J_1 = 8.6 Hz, J_2 = 4.6 Hz, 1H, Ar-H), 4.06 (s, 2H, $NHNH_2$), 4.00 (t, J = 6.6 Hz, 2H, OCH_2), 2.24 (s, 3H, Ar-CH_3), 1.81 (quin, J = 7.0 Hz, 2H, OCH_2CH_2), 1.47 (quin, J = 7.6 Hz, 2H, $OCH_2CH_2CH_2$), 1.35-1.19 (m, 18H, $OCH_2CH_2(CH_2)_9$), 0.88 (t, J = 6.8 Hz, 3H, CH_3).

d. Preparation of N-(4-n-dodecyloxy-3-methylbenzoyl)-N′-(4-(4′-n-dodecyloxy-3′-methylphenyl)benzoyl)-hydrazine (MB-MPB-22):[S3] 4-(4′-*n*-dodecyloxy-3′-methylphenyl)benzoic acid (0.58 g, 1.08 mmol) was dissolved in dry toluene (20 mL), to which thionyl chloride (0.10 mL, 1.4 mmol) and three drops of DMF were added and refluxed at 80 °C for 2 h under N_2 atmosphere. After cooled to room temperature, the remaining thionyl chloride and solvent were removed thoroughly under a reduced pressure to give the acid chloride, to which 20 mL of dry toluene was added to give a solution. 4-*n*-dodecyloxy-3-methylbenzoylhydrazide (0.51 g, 1.1 mmol) and DIPEA (0.11 mL, 0.63 mmol) were dissolved in 20 mL of dry toluene, to which the above solution

was slowly added dropwise for 15 min while heating and stirring. The solution was further refluxed at 70 °C for 2 h. After cooling to room temperature, a white precipitate was collected. The product was recrystallized from THF containing a small amount of water once and from toluene containing a small amount of acetone once, and dried at 60 °C under vacuum for 21 h, yielding 0.354 g (0.356 mmol, 33 %).

^{1}H NMR (400 MHz, $CDCl_3$): δ 9.17 (d, J = 6.8 Hz, 1H, N−H), 9.04 (d, J = 7.2 Hz, 1H, N−H), 7.89 (d, J = 8.4 Hz, 2H, Ar−H), 7.70 (d, J = 8.8 Hz, 1H), 7.67 (s, 1H, Ar-H), 7.65 (d, J = 8.0 Hz, 2H, Ar−H), 7.41 (s, 1H, Ar−H), 7.40 (s, 1H, Ar−H), 6.89 (d, J = 9.2 Hz, 1H, Ar−H), 6.85 (d, J = 8.0 Hz, 1H, Ar−H), 4.03 (t, J = 6.4 Hz, 2H, OCH_2), 4.02 (t, J = 6.6 Hz, 2H, OCH_2), 2.29 (s, 3H, Ar-CH_3), 2.26 (s, 3H, Ar-CH_3), 1.83 (quin, J = 7.0 Hz, 4H, OCH_2CH_2), 1.56-1.42 (m, 4H, $OCH_2CH_2CH_2$), 1.42-1.21 (m, 72H, $OCH_2CH_2CH_2(CH_2)_{18}$), 0.88 (t, J = 7.0 Hz, 6H, CH_3).

Elemental Anal. Calcd for $C_{65}H_{108}N_2O_4$: C, 79.78; H, 10.96; N, 2.82. Found: C, 79.47; H, 10.74; N, 3.01 %.

References for SI[§]

§ References for MEM and quantum chemical calculations (DFT and NCI) are given in the main text.

[S1] S. Kutsumizu, Y. Yamada, T. Sugimoto, N. Yamada, T. Udagawa, Y. Miwa, *Phys. Chem. Chem. Phys.*, 2018, **20**, 7953–7961.

[S2] (a) A. Suzuki, *Angew. Chem. Int. Ed.*, 2011, **50**, 6723–6737; (b) L. Liu, W. Wang, C. Xiao, *J. Orgmetallic Chem.*, 2014, **749**, 83–87.

[S3] S. Kutsumizu, S. Miisako, Y. Miwa, M. Kitagawa, Y. Yamamura, K. Saito, *Phys. Chem. Chem. Phys.*, 2016, **18**, 17341–17344.